RESEARCH

UDOT

Keeping Utah Moving

Utah Department of Transportation - Research Division
4501 South 2700 West - P.O. Box 148410 - SLC,UT 84114-8410

Report No. UT-21.05

DATA-BASED TESTING & DECISION PROCESS FOR TRAFFIC SIGNAL STEEL REPLACEMENT

Prepared For:

Utah Department of Transportation
Research & Innovation Division

Final Report
February 2021

DISCLAIMER

The authors alone are responsible for the preparation and accuracy of the information, data, analysis, discussions, recommendations, and conclusions presented herein. The contents do not necessarily reflect the views, opinions, endorsements, or policies of the Utah Department of Transportation or the U.S. Department of Transportation. The Utah Department of Transportation makes no representation or warranty of any kind, and assumes no liability therefore.

ACKNOWLEDGMENTS

The authors acknowledge the Utah Department of Transportation (UDOT) for funding this research, and the following individuals from UDOT on the Technical Advisory Committee for helping to guide the research:

- Mark Taylor
- Jesse Sweeten
- Jeremy Price
- Adam Lough
- James Corney
- David Townsend
- Mike Wright
- Mark Daniels
- Vincent Liu

TECHNICAL REPORT ABSTRACT

1. Report No. UT-21.05	2. Government Accession No. N/A	3. Recipient's Catalog No. N/A
4. Title and Subtitle DATA-BASED TESTING & DECISION PROCESS FOR TRAFFIC SIGNAL STEEL REPLACEMENT		5. Report Date February 2021 6. Performing Organization Code
7. Author(s) Andrew D. Sorensen, Ikwulono David Unobe, Brennan Bean		8. Performing Organization Report No.
9. Performing Organization Name and Address Utah State University Department of Civil and Environmental Engineering 4110 Old Main Hill Logan, UT 8432204110		10. Work Unit No. 5H08443H 11. Contract or Grant No. 18-8414
12. Sponsoring Agency Name and Address Utah Department of Transportation 4501 South 2700 West P.O. Box 148410 Salt Lake City, UT 84114-8410		13. Type of Report & Period Covered Final Feb 2018 to Feb 2021 14. Sponsoring Agency Code PIC No. UT16.305
15. Supplementary Notes Prepared in cooperation with the Utah Department of Transportation and the U.S. Department of Transportation, Federal Highway Administration		

16. Abstract

A process to estimate the fatigue damage and life expectancy of traffic signal structures under wind loads is presented. Wind speed histories of locations, where these structures are installed, are developed using wind speed data from stations located around the state. These speeds are used in computing fatigue damage at the welded connections at the base of the mast arm and pole, under the assumption that these connections are susceptible to fatigue damage. The fatigue life expectancies of these structures are thus computed. A remote monitoring application is developed using this process. This application is developed to allow operators to remotely obtain an overview of the health of these structures while in service and allow them to make informed decisions and plans with regard to repairs or retrofitting for these structures. Results from using the process on several traffic poles around Logan, Utah, indicate that most of the traffic structures are not in any immediate danger of failing from fatigue damage. However, this is with respect to some simplifying assumptions made about the welded connections and the geometry of the structures. This study aims to assist the Utah Department of Transportation (UDOT) in developing a risk assessment and management plan to properly manage traffic structures and reduce catastrophic failures or collapses.

17. Key Words Traffic pole fatigue, wind load analysis		18. Distribution Statement Not restricted. Available through: UDOT Research Division 4501 South 2700 West P.O. Box 148410 Salt Lake City, UT 84114-8410 www.udot.utah.gov/go/research		23. Registrant's Seal N/A
19. Security Classification (of this report) Unclassified	20. Security Classification (of this page) Unclassified	21. No. of Pages 58	22. Price N/A	

TABLE OF CONTENTS

LIST OF TABLES

LIST OF FIGURES

UNIT CONVERSION FACTORS

Units used in this report all conform to the UDOT standard unit of measurement (U.S. Customary System).

LIST OF ACRONYMS

AASHTO	American Association of State Highway and Transportation Officials
FHWA	Federal Highway Administration
UDOT	Utah Department of Transportation

EXECUTIVE SUMMARY

Wind speed data were collected from a variety of weather stations located in and around the Cache Valley region of Utah. The data were cleaned and analyzed to extrapolate the wind speeds expected to occur in locations where traffic signal structures are installed around the county. Several processes were applied to the collected wind speeds to remove aberrations in the data and ensure that the wind speed records were a reasonable depiction of what would occur at each site over time. These records were used to estimate the amount of time each year that the wind is expected to blow at various speeds in the eight cardinal/intercardinal directions. Estimates of the wind speed/direction profile at each traffic signal structure location were obtained by taking weighted averages of the observed profiles at nearby weather stations, with greater consideration being given to stations that are geographically closer to the traffic pole.

The wind speeds were then transformed into wind pressures using standard AASHTO-defined procedures. These pressures are converted into wind forces acting on the different parts of the traffic structures including the mast arm, fixtures, and poles. Stresses from these forces on the base connection between the pole and base plate were computed. The stresses were computed at this location as prior research has shown this to be the most vulnerable location to cyclic stresses from wind loads which create fatigue damage. The fatigue damage was computed via the Palmgren-Miner rule for cumulative damage using the time the winds are expected to have been acting on the structure and the resulting stresses from these wind speeds. Compilation of the fatigue damage from winds that these structures have endured allowed for estimations of the in-service state of the structures with respect to their remaining fatigue lives.

A monitoring tool was developed for the traffic poles around the county using the procedure outlined. This tool will allow for remote monitoring of the prevailing states of the different traffic structures, keeping operators well informed on the serviceability of these structures, allowing for a determination of which ones require closer attention over time. Some results of using this tool for traffic poles around Logan, Utah, indicate that most of the traffic structures are in a good state and should not be expected to fail from wind loads in the near future. However, a caveat to this is that the data used is purely for cyclic wind loads and as such does not take into consideration the intermittent extreme winds nor the gusts from passing vehicles, both of

which could accelerate the damage to this critical connection. Also, all welded connections are assumed to be flawless at installation but this may not be the case as weld quality could vary greatly, resulting in welded joints with small imperceptible cracks when installed which could also precipitate fatigue damage.

Overall, the tool serves as a guide to the fatigue damage occurring on these structures over time and should allow for perfunctory knowledge of the damage caused by winds on the structures over their time in service.

1.0 INTRODUCTION

1.1 Problem Statement

Fatigue damage to traffic signal structures due to repetitive wind loading can have catastrophic consequences for safety and reliability of traffic infrastructure. Such failures will negatively impact travel networks and pose a significant threat to public safety. Limiting these failures requires a plan to both monitor and track the structural health and life cycle of the traffic poles in service.

1.2 Objectives

The primary objective of this research project is to develop a risk management plan to manage traffic signal pole assets in the State of Utah in order to prevent catastrophic failures that negatively impact traffic and pose a threat to public safety.

1.3 Scope

The above objectives will be accomplished through a phased approach. The following major tasks are anticipated for each of the phases:

Phase I: Method Development and Validation

1. Literature Review

   Synthesize national literature on wind fatigue of traffic signal structures, nondestructive testing of traffic signal structures, and traffic signal asset management techniques.

2. Signal Structure Information Gathering

   In coordination with UDOT, a sample test district will be selected and information on traffic signal structures within that district will be gathered. From the information gathered,

the signals will be pooled into groups, and representative samples for each group will be selected for instrumentation and monitoring.

3. Monitoring

   Utilizing the results of the literature review, a process will be developed for computing fatigue damage to the traffic poles from the historical wind data. This process will be incorporated into a wind monitoring tool which can be used in continually keeping track of the state of the traffic signal structures.

Phase I Deliverables:

I-a: Literature Review State of the Practice Technical Paper (see Task 1).
I-b: Interim Phase I Report (see Tasks 1 and 2).
I-c: Final Phase I report (see Tasks 3 and 4).

1.4 Outline of Report

Section 2 of this report contains a review of relevant literature, covering published studies on traffic signal structures, including their response to cyclic loads, fatigue damage, weld quality and nondestructive evaluation of these structures. After reviewing the literature, a methodology for the estimation of fatigue damage of these structures from wind loads is presented in Sections 3 and 4. Section 3 discusses the collection of wind data from wind stations around Cache County. The process involves cleaning this data and then extrapolating wind speeds at locations where traffic structures are installed. Section 4 details the computation of stresses and ultimately fatigue damage from loads associated with the wind speeds. This section also presents an application developed for remote monitoring of these traffic structures for fatigue damage, using the wind speed histories gleaned from the historic wind data. Section 5 draws conclusions from the findings of this study and presents the limitations of the study, while Section 6 offers some recommendations to extend the work carried out in this study.

2.0 LITERATURE REVIEW

2.1 Overview

Ancillary structures play a critical role in the functionality of the entire transportation system by supporting highway signs, signals, and luminaires, helping to ensure safe travel for commuters and improve the robustness of the entire system over time. The American Association of State Highway and Transportation Officials' (AASHTO) Load and Resistance Factor Design (LRFD) specifications (AASHTO-LRFD 2016) recognize four types of ancillary structures: sign support structures, luminaire support structures, traffic signal support structures, and their combinations. Although the AASHTO specifications provide thorough design specifications for ancillary structures, they are less detailed on procedures for inspection and management of these structures. Consequently, to bridge this code limitation, research studies on the fatigue life of ancillary structures and the need for periodic inspection of these structures have been conducted. A body of literature resulting from these studies forms the basis for current practices in management and inspection of ancillary structures. This report provides a review of published research on fatigue behavior and in-service inspection and management of ancillary structures.

Initially, a background on the fatigue behavior of ancillary structures and the contributing loads is presented. This is followed by a review of research on fatigue susceptibility, asset management, and nondestructive evaluation (NDE) of sign structures, showing the promise displayed by nondestructive evaluation methods in enhancing the service life of these structures. Finally, a short description of various state Department of Transportation (DOT) inspection manuals for the management of sign structure assets is provided.

2.2 Fatigue

The continual cyclic loading of wind on slender structures leads to the susceptibility of these structures to accumulation of fatigue damage and could eventually lead to fatigue failure of these structures (Ginal 2003). Fatigue failures are the most common type of failure for ancillary structures. For this reason, the fatigue life of these structures is of great importance. Infinite fatigue life of a structure is described as when the nominal stress (Δf) near fatigue-prone areas is less than the constant amplitude fatigue threshold, $(\Delta F)_{TH}$ (AASHTO-LRFD 2016). To determine the

infinite fatigue life of a structure, AASHTO recommends using a static wind pressure of 277.5 Pa (5.8 psf). The values of $(\Delta F)_{TH}$ are provided by AASHTO (AASHTO-LRFD 2016). If Δf is greater than$(\Delta F)_{TH}$, the nominal stress is recalculated by applying a static wind pressure of 62.2 Pa (1.3 psf). Then, using the fatigue detail category constant (A), the total number of cycles (N) before fatigue failure occurs is calculated as shown in Equation 2.1.

$$N = \frac{A}{(\Delta f)^3} \tag{2.1}$$

According to Equation 2.1, areas with larger values of A have more fatigue life. For instance, groove-welded connections have more fatigue life than fillet welded connections. These values of A are dependent on the connection detail type.

To find the remaining fatigue life of an ancillary structure, the number of fatigue cycles induced by wind per day (N_{day}) is first determined. The AASHTO values for N_{day} are based on the mean annual wind speed of the location of the structure. The cycles range from 9,500 to 23,000 for mean wind speeds of 14.5 km/h (9 mph) to 17.7 km/h (11 mph), respectively.

The specific use of extreme static wind loads for the design of these structures is not sufficient for the design of stationary structures (Barle et al., 2011). Fatigue evaluation and fatigue life prediction carried out for a fractured structure based on the estimated stress spectra and allowable stresses in the corresponding design code using finite element analysis, found that sole use of static pressure, even amplified values, is not always adequate for fatigue design (Barle et al., 2011). As such, the peculiarities of the interaction between wind loads and ancillary structures need to be better understood to adequately discern the fatigue life of the structures.

2.3 Wind Load on Sign Structures

Wind loads are primarily the effects of moving air on structures, often caused by natural wind or passing vehicles (especially large vehicles such as semi-trucks), and are primarily responsible for occurrences of fatigue crack in ancillary structures. There have been several studies done to find the effective wind pressure on the supporting structures. The studies have shown that there is an intrinsic relationship between the source/type of wind load and the structural response, which could lead to inadequacies in design specifications that do not consider some of the types of fatigue-stress-inducing wind loads in ancillary structures. These wind load types include natural

wind (natural wind, vortex shedding, and/or galloping) and vehicle-induced gusts. In this section, a brief review of current literature on wind loads and their effect on fatigue design of sign structures is presented.

2.3.1 Natural Wind

A necessary loading scenario for ancillary structures, natural wind is sometimes difficult to quantify as a load due to the existence of secondary loading conditions such as vortex shedding and galloping (Ginal 2003). While natural wind produces forced vibrations on structures, these secondary conditions initiate and enhance self-excited vibrations in the structure.

A number of studies on natural wind conducted to more accurately design ancillary structures against fatigue have concentrated on determining adequate equivalent static wind pressures, which are used to simulate wind conditions in designing structures. These studies, utilized field data and simulations to make many observations about the effects of natural wind on ancillary structures, which have proven useful in understanding the fatigue response of these structures. Some of these observations include classifying loads as having an Extreme Type III distribution (South 1994), meaning wind speeds exceeding the design speeds in the AASHTO specifications (Connor 2012), defining areas of the structures as particularly vulnerable to wind loads (Dexter and Johns 1998; Kaczinski et al., 1998; Li et al., 2006), and determining the types of wind load most likely to induce fatigue in ancillary structures (Dexter and Johns 1998; Kaczinski et al., 1998; Li et al., 2006). Some recommendations were made to mitigate the fatigue stresses in ancillary structures from natural wind including changes to recommended wind loads (Dexter and Johns 1998; Kaczinski et al., 1998; Li et al., 2006), varying equivalent static forces to account for geographical peculiarities (Connor 2012), avoidance of fatigue susceptible details (Kaczinski et al., 1998; Li et al., 2006), and some measures to reduce wind-induced vibrations in the structures (Kaczinski et al. 1998).

2.3.2 Vortex Shedding

Vortex shedding involves the circular movement of fluids coming off a solid surface. A secondary effect of moving air flowing past bluff bodies such as traffic ancillary structures, vortex

shedding is characterized by the formation of vortices at the back of the body, which cause vibrations in the body that could lead to damaging cyclic loads.

An important factor that contributes to vortex shedding is lock-in speed. Lock-in occurs as the vortex shedding frequency nears the natural frequency of vibration of the structure (DeSantis and Haig 1996). DeSantis et al., (DeSantis and Haig 1996) utilized finite element analysis of a structure to determine the critical wind velocity for lock-in speed and found this to be only 2.16 km/h (1.34 mph).

Some studies carried out to determine the effects of vortex shedding on ancillary structures concluded that vortex shedding is responsible for large amplitude vibrations in these structures at low wind speeds (Edwards and Bingham 1984; Kaczinski et al., 1998; McDonald et al., 1995; Zuo and Letchford 2010). Although these studies concluded with diverging views on the significance or otherwise of vortex shedding on the fatigue behavior of these structures, they generally agree that its effects are greatly reduced when the ancillary structure has enough attachments on it to distribute the vortex formation. Other studies also determined that vortex-shedding-imposed vibrations are less critical than those of natural wind and as such cannot be considered critical (Ginal 2003; Li et al., 2006). A way to mitigate vortex shedding is by reducing the periodicity of vortex formation or reducing the spanwise cohesiveness of the flow (Pulipaka et al., 1998). Some studies concentrating on this method have recommended different approaches to achieve this including using a perforated cylinder around a plain cylinder (Price 1956), triangular spoilers on a suspended pipeline (Baird 1955), and helical strakes on vertical stocks (Scruton and Walshe 1957).

2.3.3 Galloping

Galloping refers to the flow-induced vibration of a structure, occurring due to the oscillation of wind flow around the structure relative to its motion, (Pulipaka et al., 1998) and is primarily caused by the aerodynamic instability of a structure.

Field measurements and finite element analyses of inverted L-shaped cantilever structures in California for fatigue failure revealed galloping instability to be the cause of the failures, with measured and effective stresses from galloping at 137.8 MPa and 81.3 MPa respectively, exceeding the design values provided by AASHTO Section 2 (Gilani and Whittaker 2000a).

For ancillary structures, the occurrence of galloping is highly dependent on structural characteristics including its cross section, total damping ratio and natural frequencies as well as

certain flow characteristics such as turbulence intensity. Requiring a number of these parameters to be aligned in order for aerodynamic instability to occur and galloping to take effect, this loading scenario occurs rarely and as such, need not be considered in designing traffic sign support structures (Ginal 2003). Other studies measuring the effective design load for galloping agree that although galloping does cause large oscillations in sign structures, it is not an important source of vibration causing fatigue damage in most types of ancillary structures (Fouad et al., 2003; Kaczinski et al., 1998; Li et al., 2006).

However, this observation comes with a caveat. The circular cross section of the structural members that make up traffic signal structures are not susceptible to galloping instability as circular cylinders always experience positive aerodynamic damping, but galloping may occur due to the features of the signs and signal attachments on the mast arm and as such cannot be overlooked (Kaczinski et al., 1998).

Methods recommended to mitigate galloping include installing dampers (tuned mass dampers, liquid-tuned dampers, spring/mass friction dampers), changing the conjugation, and/or removing the back plate.

2.4 Vehicle-Induced Wind Loads

Vehicle-induced wind loads on ancillary structures encompass all types of wind gusts generated by moving vehicles that produce displacements on the structures. Studies to establish the effects of vehicle-induced pressure gusts on sign support structures have led to divergent conclusions as to the importance of such loads on the fatigue behavior of the sign structures. Such conclusions range from vehicle-induced loads being insignificant to the fatigue phenomena (Albert 2006; Creamer et al., 1979; Ginal 2003) to being significant enough to include in the design criteria (DeSantis and Haig 1996; Dexter and Johns 1998; Edwards and Bingham 1984; Johns and Dexter 1999; Kaczinski et al., 1998). Such discrepancies can be attributed to some varying factors in case studies including height of the structures above the roadway (Cook et al., 1996), quality of workmanship and material characteristics (Gilani et al., 1997) and vehicle shape (Cali and Covert 2000).

The latest version of the AASHTO manual for ancillary structures (AASHTO-LRFD 2016) uses fatigue importance factors to evaluate fatigue design loads. Fatigue design loads ranging from

0.30 to 1.0 are used for different fatigue categories, structure types (cantilevered or un-cantilevered), and different wind loads (galloping, natural wind, and vehicle induced). The product of the basic pressure, importance factor, and drag coefficient (only for natural wind and vehicle-induced gusts) are considered as the fatigue design load by this manual. The base fatigue design pressure for galloping applied vertically is 1 kPa (21 psf), for natural wind gusts applied horizontally is 248.8 Pa (5.2 psf), and for truck-induced loads applied vertically is 899.5 Pa (18.8 psf). For high-mast lighting towers, the basic pressure provided by Connor (Connor 2012) is used.

As enumerated in this section, a number of studies have attempted to characterize the response of ancillary structures to wind loads and gauge their long-term fatigue behavior. A review of these past studies shows significant uncertainties regarding wind loads on ancillary structures. Different conclusions were reached with regard to the importance or otherwise of the different wind loading scenarios and several recommendations made as to an ideal design load for ancillary structures. These results are summarized in Table 2.1 below.

Table 2.1 Basic Fatigue Design Pressure Due to Wind

Source	Structure Type	Load Type	Direction	Pattern	Magnitude, kPa (psf)
Creamer et al. (1979)	Cantilever Sign Support	Truck-Induced	Vertical & Horizontal	Triangular	0.059 (1.23)
		Truck-Induced	Vertical & Horizontal	Constant	0.060 (1.25)
Edwards and Bingham (1984)	Cantilevered Truss Sign Support	Truck-Induced	Vertical & Horizontal	Triangular	0.067 (1.41)
Johns and Dexter (1998) and (1999)	Cantilevered VMS	Natural Wind	Horizontal	Constant	0.249 (5.2)
Kaczinski et al. (1998)	Cantilevered Signs, Signals, and Light Support	Natural Wind	Horizontal	Constant	0.249 (5.2)
Fouad, et al. (2003)	Un-cantilever	Galloping	Vertical	Constant	1.00 (21)*
	Cantilever	Natural Wind	Horizontal	Constant	0.249 (5.2)*
	Cantilever	Truck-Induced	Vertical	Constant	0.488 (10.2)*

Li et al. (2006a)	Cantilever	Galloping	Vertical	Constant	1.00 (21)*
	Cantilever	Natural Wind	Horizontal	Constant	0.249 (5.2)*
	Cantilever	Truck-Induced	Vertical	Constant	1.75 (36.6)*
Connor (2012)	High-Mast Lighting Towers	Natural Wind	Horizontal	Constant	0.278 (5.8)* 0.311 (6.5)* 0.344 (7.2)*
AASHTO (2013)	All	Galloping	Vertical	Constant	1.00 (21)*
	All	Natural Wind	Horizontal	Constant	0.249 (5.2)*
	All	Truck-Induced	Vertical	Constant	0.900 (18.8)*
	High-Mast Lighting Towers	Natural Wind	Horizontal	Constant	0.249-0.344 (5.8-7.2)
DeSantis et al. (1996)	Cantilever	Truck-Induced	Vertical	Constant	1.27 (26.5)*

Note: * Basic pressures

These results show that there are some divergent views as to an ideal design pressure that will adequately characterize wind loads on ancillary structures. These divergent results can be attributed to some factors that vary between the different studies. These factors include some location-dependent wind characteristics as well as the structural characteristics of the different ancillary structure configurations studied.

2.5 Wind Characteristics

From the data collected and resulting analyses in several studies, some characteristics of wind flow and surrounding environment have a significant impact on the wind loading phenomena determined to be principal sources of fatigue-inducing stresses in ancillary structures. These characteristics include wind speed, direction, and topography of the surrounding areas. As such, understanding the role of these characteristics is important in fatigue design of ancillary structures.

A study of overhead structures above roadways determined that wind speed plays a major role in the fatigue behavior of ancillary structures with the majority of fatigue damage occurring at wind speeds over 25 mph and none at wind speeds below 15 mph (Ginal 2003). This study also established that wind direction plays a critical role in the fatigue behavior of some configurations of overhead sign structures, particularly tri-chord structures. Another study to understand the role

of wind characteristics in the fatigue behavior of traffic signal structures concluded that topography has a significant effect on the one-hour average wind speed but minor effect on the wind direction. Wind speeds imposed on sign structures in urban and suburban terrains were found to be much less than those in flat terrains (Diekfuss 2013). The study concluded that in order to obtain more realistic wind models, the topographical effect of the sign support structure locations and the wind speeds should be combined to effectively determine the effect of natural wind on these structures.

2.6 Structure Characteristics

Some studies on the effects of structural characteristics on the resultant stresses on ancillary structures from wind loads indicated that geometric configurations have a telling effect on the structures' response to wind forces. Some of these include open-sided models which are more vulnerable to wind-induced torque than single plate signs (Zuo et al., 2014), as well as clearance and aspect ratios significantly influencing the resultant wind-induced loads on ancillary structures (Zuo et al., 2014).

Another characteristic of the structure that plays an important role in its fatigue behavior is its damping ratio. A study carried out to determine the effect of damping ratios on highway sign structures instrumented and collected data from three cantilevered highway structures (Creamer et al., 1979). This study consequently determined the fundamental vibration modes and critical damping ratios for this type of sign structure. The calculated horizontal and vertical damping ratios were 0.4% to 1.11% of the critical damping ratio (Creamer et al., 1979). The study opined that this low damping ratio is one of the reasons that ancillary structures are vulnerable to wind loads as more stress cycles are produced for a given load, consequently decreasing the stress range required to produce fatigue failure (Creamer et al., 1979). A later study also found the critical damping ratios to be similarly small with values between 0.25% and 0.57% (Dexter and Johns 1998). Other studies indicated that low damping ratios increased the fatigue susceptibility of ancillary structures (Chavez et al., 1997; Irwin and Peeters 1980). The damping ratios of different ancillary structures that have been studied over time is shown in Table 2.2.

Table 2.2 Damping Ratios

Source	Structure Type	Sign Type	Damping Ratio
Creamer et al. (1979)	Cantilevered pipe truss supported by mono-tube	Aluminum	0.4 - 1.11
Edwards and Bingham (1984)	Two-chord and four-chord cantilevered pipe truss supported by mono-tube	Aluminum	0.58 - 1.85
Johns and Dexter (1998, 1999)	Two-chord cantilevered pipe truss supported by mono-tube	VMS (variable message sign)	0.25 - 0.57
Kaczinski et al. (1998)	Cantilevered sign and signal support structures	Aluminum	0.12 - 0.62
Gilani et al. (1997)	Mono-tube cantilever mast arm	VMS (variable message sign)	0.5 - 0.7
South (1994)	Cantilevered mono-tube mast arm and upright traffic signal	Aluminum	0.6

Investigations into fatigue failure of ancillary structures have isolated certain areas of the structures to be particularly prone to fatigue failure (Chen et al., 2003; DeSantis and Haig 1996; Kaczinski et al., 1998). Of particular interest are connections between members, especially welded connections as they seem to be the most susceptible to such damage. In traffic signal structures, this would be principally at the mast-arm-to-baseplate and pole-to-baseplate connections.

Typically fatigue failures occur when wind or truck-induced loads exceed the capacity of the connection or member. Premature failures in the ancillary structures are caused by stress in the welds being higher than the design stress, the number of cycles exceeding expectations, or substandard weld quality.

Weld quality has been shown to cause the majority of failures. The welds with undercut defects are prone to failure initiation, which leads to cracking in the heat-affected zones in the base metal. Laboratory tests to determine the variation in weld quality across manufacturers showed two out of three mast arms made by one manufacturer and two out of two mast arms made by another manufacturer failing prematurely due to poor weld quality.

With welding being the primary method used in connecting different parts of ancillary structures, the focus on fatigue resistance of these structures has primarily been on the connections within the structure's framework.

Studies on the relationship between the connections and fatigue behavior of these structures determined that the response of the connections in ancillary structures to fatigue-inducing cyclic loading was controlled by some factors including weld sizes (Archer and Gurney 1970), position of the connection (South 1994), and weld types (Anderson 2007). Physical characteristics of the structures including presence of conduit holes, galvanizing of components, presence of stiffeners, structural shape/type, and component sizes also play an important role in the fatigue life of these structures (Alexander and Wood 2009; Anderson 2007; Chavez et al., 1997; Irwin and Peeters 1980; Kacin et al., 2010; Koenigs et al., 2003; Li et al., 2006; Peiffer et al., 2008; Xiao and Yamada 2003).

These studies made some recommendations for improving the fatigue resistance of ancillary structures. These recommendations, made in view of the observations of the factors leading to fatigue susceptibility include using thicker fillet welds at all connections (Archer and Gurney 1970), using airfoils to increase damping ratios (Irwin and Peeters 1980), drilling conduit holes as opposed to flame cutting (Chavez et al., 1997), using U-stiffeners and ring-strengtheners (Anderson 2007; Xiao and Yamada 2003), increasing base-plate thickness (Anderson 2007), and using a galvanized coating with higher toughness and less susceptibility to fatigue cracking (Alexander and Wood 2009).

These studies all highlight the inadequacies of the AASHTO specifications for fatigue-resistant design of ancillary structures prompting the modification of the specifications to surmount these shortcomings.

2.7 Fatigue Reduction

To alleviate fatigue-inducing stresses and by extension enhance the life expectancy of ancillary structures, three main methods have been recognized and used. These are increasing the stiffness, changing some in aerodynamic characteristics, and installing mechanical devices.

Several studies have indicated that one way to increase the fatigue life of ancillary structures is to mitigate the oscillations by increasing the damping ratios. This can be done by

installing dampers (Christenson and Hoque 2011; Cook et al., 2001; Hamilton III et al., 2000; Ljumanovic 2010; McManus et al., 2003) increasing damping and mass units (e.g. by using thicker walls) (Caracoglia and Jones 2004), post tensioning the structure (Koenigs et al., 2003; Wieghaus et al., 2017), and increasing plate thickness at connections (Roy et al., 2011).

Different configurations of dampers were tested across the different studies with varying degrees of success. One study found tapered impact dampers to be the most successful in reducing vibrations in both the vertical and horizontal directions (Cook et al., 2001). Another study recommended using a dual strut damper, over tuned-mass and strand impact dampers, to reduce the in-plane vibrations (McManus et al., 2003). Low-cost mass-rubber dampers are recommended to reduce bending, shear, and fatigue loading (Ljumanovic 2010) and a vibration absorber to reduce displacements (Christenson and Hoque 2011).

Increasing the damping ratio of ancillary structures mitigates oscillations, which leads to higher fatigue life. For existing structures, installing dampers has shown promising results in the lab setting. However, since damper performance is related to the site, structure type, damper type, capability, and cost, it is difficult to make a single recommendation. There are also challenges with the aesthetics of the structure which can be compromised if dampers are used. Despite considerable lab success, oscillation mitigation methods have not been widely adopted by departments of transportation to increase the fatigue life of ancillary structures. Possible reasons for this could include time, cost, and uncertainty in the frequency and pressure of wind loads

Post-tensioning the structure was found to relieve the weld connections from the fatigue-causing stresses (Koenigs et al., 2003; Wieghaus et al., 2017). Increasing the plate thickness was found to be a cost-effective way of increasing the fatigue life of the connection (Roy et al., 2011). The study recommended a 2-inch minimum thickness.

Also, a detail for unstiffened full-penetration groove-welded tube-to-transverse plate connections, with reduced openings in the transverse plates, upgraded the connections for category E to C, and is a cost-effective method of improving the fatigue life of the connection. Fillet-welded connections with an optimized stiffener size with proposed ratios of 1.25 and 1.6 for stiffener thickness to the tube thickness and stiffener height to the stiffener spacing, respectively, are also recommended as an economical, efficient fatigue-resistant detail (Roy et al., 2011).

For multi-sided tube-to-transverse plate connections, fewer sides and sharper bend corners increase the stress concentration increasing fatigue susceptibility (Roy et al., 2011). A minimum

number of eight sides and a 1-inch bend radius are suggested for multi-sided tubular structures. Handholes and other cutouts in sign support structures are recommended to be located at low stress areas. Since stress cycles are generally in the plane containing the arm, the cutouts and handholes locations should be focused on the side normal to the containing arm, with their width being limited to 40% of the tube diameter.

No fatigue cracks were observed in tests in mast-arm-to-pole connections with fillet-welded gusseted boxes or ring-stiffened boxes. The width of the box connections is proposed to be equal to the pole diameter. The ring-stiffened box is recommended in regions with expected high oscillations, while gusseted-box connections are considered satisfactory in other regions (Roy et al., 2011).

It was also observed that structures with larger spans or redundancy have more fatigue life and greater inspection intervals (Diekfuss 2013). In addition, sign mast-arm structures with more cantilever length are more prone to fatigue cracking than the high mast poles with less cantilever length (Roy et al., 2011).

2.8 Ancillary Structures' Asset Management

Designing a methodology for the management and inspection of ancillary structures involves two pertinent aspects, namely frequency of assets' inspection and the optimal method of inspection that will both accurately capture the state of the asset and can be conveniently carried out in the field. Most studies carried out regarding asset management of ancillary structures have primarily dealt with these two aspects and, in addition, some have made efforts to make recommendations to prolong the fatigue life of existing or new ancillary structures. In this section, a summary of these studies is provided.

2.8.1 Inspections

The Federal Highway Administration (FHWA) published a technical report in 2005 to provide guidance for asset management of structural support of highway signs, luminaires, and traffic signals, with a focus on addressing wind-induced vibrations and fatigue (Garlich and Thorkildsen 2005). Recommended inspection frequencies in this report were adopted by the AASHTO manual. Four types of inspections are generally recommended by AASHTO for

ancillary structures: initial (shortly after installation), routine (periodic), damage (after a major environmental incident such as storms), and in-depth (a follow-up to routine inspection for members that require more investigations) (AASHTO-LRFD 2016). A program manager is usually tasked with determining the frequency of inspections. The code recommends considering material type, condition, importance, accessibility, and allocated funds when determining the inspection frequency. **Error! Reference source not found.** shows the Federal Highway Administration (FHWA) guidelines for inspection frequency of ancillary structures as suggested by AASHTO (AASHTO-LRFD 2016).

Table 2.3 AASHTO Recommendations for Inspection Frequency of Ancillary Structures

Type	Inspection Type	Interval (Year)
Aluminum Structures	In-Depth	2
Cantilever, Butterfly, and Other Non-Redundant Structures	In-Depth	4
Typical Sign Bridges (Span)	In-Depth	6

Ancillary structures can be classified according to the estimated severity of the fatigue damage caused by wind. Class A structures, single and double mast arm structures, are more susceptible to wind-induced fatigue damages while class B structures, tri-chord and box truss overhead sign bridges, are more resilient to fatigue cracks. This can be used to determine the inspection intervals of each structure with an inspection interval of 4 years recommended for Class A structures and 8 years for Class B structures (Li et al., 2006). By this definition, traffic signal structures, the subject of this study, would fall into Class A and as such, require a 4-year inspection interval. More recently, a reliability-based study of ancillary structures proposed using a reliability-based protocol to determine the service time interval when the first inspection of the structure for fatigue damage should take place, afterwhich the recommended 4-year interval for inspections can commence. This service time will differ across structures, being dependent on some underlying factors such as detail configuration, orientation, location, and type. The research also proposed reliability-based assessment protocols as a more efficient inspection procedure for finding fatigue-induced cracks in structures (Diekfuss 2013).

2.8.2 Structure Life Expectancy

For proper assest management, it is important to know the life expectancy of an ancillary structure. A survey of various departments of transportation (DOT) concluded that the life expectancy of traffic signals' support structures is approximately 15 years (Markow 2007). **Error! Reference source not found.**2.4 shows a summary of this survey. Roadway lighting life expectancies were also investigated as shown in **Error! Reference source not found.**2.5. The major factors affecting the life expectancy of these structures are: pole/bulb type, temperature extremes, and other environmental factors.

Table 2.4 Survey of Life Expectancy Estimates for Traffic Signal Support Structures (Markow 2007)

Structural System Component	No. of Responding Agencies	Median Life Span (years)
Tubular steel mast arm	14	20
Tubular aluminum mast arm	7	20
Wood pole (and span wire)	9	15
Concrete pole (and span wire)	2	12.5
Steel pole (and span wire)	9	20
Galvanized pole and span arm	1	>100

Table 2.5 Survey of Life Expectancy Estimates for Roadway Lighting (Markow 2007)

Structural System Component	No. of Responding Agencies	Median Life Span (years)
Tubular steel	12	25
Tubular aluminum	9	25
Cast metal	2	22.5
Wood posts	2	32.5
High mast or tower	11	30

2.9 Nondestructive Evaluation of Ancillary Structures

Nondestructive evaluation (NDE) methods are the principal means of in-service inspection of ancillary structures. The basic principle of NDE is simply determining the quality or integrity of an item without altering its usefulness or functionality (Shull 2016). Irrespective of the details of the method, every NDE process consists of four primary steps, namely: application of an external stimulus, sensing and recording the response in the component of interest from the

stimulus, finding possible anomalies in the response indicating the presence of defects, and interpretation of the collected results.

There are several NDE methods used for structural health monitoring and inspection purposes, each suitable for specific materials, conditions, or defects. The most common NDE techniques used in ancillary structure inspections are visual inspection, dye-penetrant testing (PT), magnetic particle inspection (MPI), ultrasonic testing (UT), and infrared thermography (IRT). This section provides information about each of these techniques, as well as other, less common methods of inspection.

2.9.1 Visual Inspection

Visual inspection is defined as "the process of examination and evaluation of systems and components by use of human sensory systems aided only by mechanical enhancements to sensory input such as magnifiers, dental picks, stethoscopes, and the like. The inspection process may be done using such behaviors as looking, listening, feeling, smelling, shaking, and twisting" (Spencer 1996). Visual inspection is the simplest NDE method and remains the primary in-practice method for finding fatigue cracks and other defects.

Although easy in application, this method is beset by many challenges including a dependency on human factors such as level of experience and meticulousness of the inspector, as well as the ability to physically access the location of interest and the existence of surface indications of defects. Technically, visual inspection does not meet the definition of the NDE methods, but it is widely used by inspectors.

To minimize the disadvantages, training the inspectors and following the recommendations for visual inspection laid out in the "Bridge Inspector's Training Manual" is necessary (Hartle et al., 1995). Inspection manuals generally prescribe a visual inspection method for ancillary structures.

2.9.2 Penetration Testing

Penetration testing (PT) is one of the most common and least expensive NDE methods for finding defects in metal materials such as steel and aluminum. It is often used to find surface discontinuities (defects) which may not be easily visible by utilizing a low-viscosity fluid (referred

to as the penetrant) and another fluid (called the developer) to enhance the visibility of the defects. The surface to be tested is initially thoroughly cleaned to remove any surface impurities that might interfere with the test. The penetrant is then applied to the surface and allowed to seep through any discontinuities. The surface is then cleaned to remove the penetrant left on the surface without removing any that has flowed through discontinuities. The second material (developer) is then applied to the surface to draw the liquid from any cracks by capillary attraction. The developer provides a contrasting background that allows for easy visibility of any penetrant liquid thus removed and the presence of penetrant drawn to the surface indicates the presence of discontinuities (cracks) in the material (Shull 2016). Non-fluorescent penetrants are better suited for field inspections because they are easier to implement.

There are different types of penetrants, penetrant removals, and developers in use. For the field inspection of welds in sign structures, the most commonly used are the solvent-removable visible penetrant, which is portable and sensitive, but can be labor intensive and the water-washable visible penetrant which is less time-consuming, less expensive, but also less sensitive.

Initial visual inspection is required before using PT to identify candidate locations for cracks. PT inspection of sign structures needs to follow the procedure provided in ASTM E-165 "Standard Test Methods for Liquid Penetrant Examination." Although PT inspection is inexpensive and requires less skill than other commonly used NDE methods, it does have some disadvantages including only being capable of spotting surface cracks, large enough discontinuities that can allow for penetration of the penetrant, clean surfaces with nothing blocking the discontinuities or defects, and it is ineffective for sharp corners and complex shapes (Shull 2016). In addition, the results of the PT inspection can be erroneous when used for porous materials.

2.9.3 Magnetic Particle Inspection

Used for ferromagnetic materials, magnetic particle inspection (MPI) utilizes the ferromagnetic property of the metals (usually steel) to find surface or near surface defects. The process involves inducing a magnetic field in the object which can be distorted by the presence of a discontinuity, e.g., a crack. In order to visualize the magnetic field and find discontinuities, fine magnetic particles are sprayed (wet particles) or dusted (dry particles) on the test-piece, which will be attracted to the edges of any discontinuities at or slightly below the surface, revealing the

presence of the discontinuity. For fine cracks, wet particles are more effective and dry particles perform better on rough surfaces and for subsurface defects.

After an initial visual inspection is carried out, MPI can be used for further investigation of regions deemed to require closer inspection. The MPI procedure is defined in ASTM E-709, "Standard Guide for Magnetic Particle Examination." This method is generally low cost, simple to operate, offers easy interpretation of results, can be automated, and provides some information on the depth of defect (Shull 2016). However, some downsides of MPI include only being useful on ferromagnetic materials, limited ability to detect subsurface defects, and it is time consuming (Shull 2016). Also, the application of MPI for weld inspection can be limited due to its ineffectiveness for rusty and jagged surfaces.

2.9.4 Ultrasonic Testing

One of the most widely used NDE methods, ultrasonic testing (UT), is generally utilized as a follow-up to visual inspections of the ancillary structures for areas deemed to require an in-depth investigation. UT is usually used for subsurface defect detection and should be performed in accordance with ASTM E-164, "Standard Practice for Ultrasonic Contact Examination of Weldments."

The process employs the theory of wave propagation, particularly that of ultrasonic waves through solids. Ultrasonic waves of frequencies between 50 kHz to several gigahertz are applied to the test piece in various surface locations through a set of ultrasonic transducers. The waves are received at other locations where the wave propagation and travel time are recorded. In locations with subsurface defects, the propagation path of the sound waves is changed, and this can be used to identify the defects, their locations, and sizes (Shull 2016). UT is often used to confirm visually detected fatigue cracks at the end of the horizontal gusset plate connections in sign structures (Cook et al., 2000).

UT is a very useful NDE technique as it is very sensitive to minute discontinuities, is very quick, accurate, and portable, can be used on most materials, and can be automated. It does have a few disadvantages however, requiring a high level of skill and training for implementation and interpretation as well as being expensive and insensitive to planar flaws perpendicular to the wave front (Shull 2016).

2.9.5 Infrared Thermography

Infrared thermography (IRT) involves the use of an infrared camera in combination with an external stimulus to analyze the thermal response of an object to the stimulus. Infrared images of the surface are analyzed to extract information on the temperature of the surface, and this is used to recognize the presence of subsurface defects or anomalies due to a variation in the thermal properties at such locations from that of the rest of the surface. Infrared thermography is an effective NDE method to detect not only subsurface defects, but also surface defects such as cracks. Different excitation methods have been tested for fatigue crack detection in materials including laser (An et al., 2014), radiography (Lahiri et al., 2011), and electrical current (Vrana et al., 2008).

IRT provides a practical method for real-time detection of defects in structures and can be used for a wide array of materials with little or no contact with the surface under investigation. It also lends itself well to possible automation of the evaluation process (Garrido et al., 2018). However, some disadvantages of IRT as a nondestructive evaluation method include high initial cost of equipment and lower accuracy of temperature reading from infrared cameras compared to contact methods such as thermocouples (Garrido et al., 2018).

Other types of NDE methods may be used for fatigue crack detection and monitoring. These include Electrochemical Fatigue Sensor (EFS) and fatigue fuse. Electrochemical Fatigue Sensor (EFS) is a short-term testing and inspection system, produced by Metal Fatigue Solution (MFS), consisting of RETROCHEK and CRACKCHEK. This equipment can be attached to the structure to determine the growth of an existing crack or to detect the presence of microplasticity (precursor to crack growth) in susceptible regions ("Metal Fatigue Solutions^{TM}" n.d.). Another device produced by MFS is a fatigue fuse. A fatigue fuse is a thin metal piece comprised of a series of parallel metal strips connected to a common base. When a fatigue crack reaches a certain point of its life expectancy corresponding to the weakest strip of the fuse, that strip will break. As the crack grows, more strips will be broken, giving this device crack monitoring abilities ("Metal Fatigue Solutions^{TM}" n.d.).

2.9.6 Current DOT Ancillary Structures' Inspection Manuals

It is common for a state's Department of Transportation (DOT) to publish manuals and outline their own standards for the inspection of ancillary structures. The recommended duration for inspection of sign structures varies by state and is specified in their inspection manuals. This variance can be attributed to the unique conditions present for traffic ancillary structures at different locations as well as the variations in the designs of these structures. Table 2.6 gives a summary of the recommended inspection types and durations from the different studies and department manuals available.

Table 2.6 Summary of Ancillary Structures' Inspection in United States' DOTs

Structure	Type of Inspection	Interval (Years)
Li et al. (2006)		
Single mast arm	Routine	4
Double mast arm	Routine	4
Tri-chord bridge	Routine	8
Box-truss bridge	Routine	8
Mon-tube	Routine	8
KDOT 2014		
Sign and High Mast Structures	Hands-On	4
NYSDOT 2013		
Cantilever	Type1*	4
Cantilever	Type2*	2
Span	Type1*	6
Span	Type2*	3
High mast	Type4*	4
General	Type3*	1
Oregon DOT		
Mast Arm and Poles [a]	Visual & Galvanizing Thickness Measurement	Owner Choice
Mast Arm and Poles [b]	Visual	Owner Choice
VDOT 2014		
Cantilever	Regular**	4
Overhead Span	Regular**	6
Sign Butterfly	Regular**	4
Sign VMS/CMS, Cantilever	Regular**	4
Sign VMS/CMS, Span	Regular**	6
Sign, Bridge Parapet Mounted	Regular**	2
High Mast	Regular**	4
FDOT 2014		
High Mast	According to FHWA	5
Overhead	According to FHWA	2

Ohio		
OH [c] Sign/Signal, High Mast	Regular***	5
Bridge Mounted	Regular***	1
NC DOT 2018		
Cantilever	In-Depth	4
Span	In-Depth	8
High Mast	In-Depth	5

Note: [a] Built Before 1980
[b] Built After 1980
[c] OH=Overhead
*Refer to the New York DOT section for definitions
**Refer to the Virginia DOT section for definitions
***Refer to the Ohio DOT section for definitions

2.10 Summary

Wind loads due to natural wind gusts, truck-induced gusts, and galloping are the main cause for fatigue formation in ancillary structures. Vortex shedding is rarely observed in ancillary structures and has been omitted in most past studies of fatigue design. Based on the literature review of past studies carried out on ancillary structures, the following observations have been made on the fatigue performance of ancillary structures.

- Using damping and removing the back plates mitigates galloping (Gilani and Whittaker 2000b; McDonald et al., 1995);
- The majority of past fatigue failures have occurred in the mast-arm-to-column, the column-to-baseplate, and/or the anchor bolts (Kaczinski et al., 1998);
- Vortex shedding rarely occurs in ancillary structures including traffic signal structures (Kaczinski et al., 1998; Li et al., 2006);
- Natural wind and truck-induced gusts cause most of the fatigue cracks in cantilevered structures (Kaczinski et al., 1998);
- The concrete jacket can be used to increase the damping ratio and mitigate the oscillations (Gilani and Whittaker 2000b);
- There is linearity between truck events and the stress range (Ginal 2003);
- Weld under-cut can cause premature failures in ancillary structures (Chen et al., 2003);
- Shot peening can be used to add comprehensive residual stress on the weld surface with under-cut to improve fatigue life (Chen et al., 2003);

- The anchor rods, strut-to-gusset plate welded connection, and gusset plate-to-chorded weld connections have infinite fatigue lives regardless of the structural type of cantilever structure (Li et al., 2006);
- Chord-to-transverse-plate weld connections are prone to fatigue cracks in box-truss sign structures (Li et al., 2006);
- Post-to-base weld connections are prone to fatigue failure for the tri-chord sign structures (Li et al., 2006);
- Galloping causes the most vibrations in a single mast arm cantilever (Li et al., 2006);
- Regions with the highest stress concentrations (critical locations in terms of stress range) in sign structures are mast-arm-to-flange plate, connection bolts, and below the box connections (Peiffer et al., 2008);
- Swage joints in the poles are prone to fatigue cracks (Alexander and Wood 2009);
- Diagonal members in truss sign structures experience more severe stresses (Kacin et al., 2010; Peiffer et al., 2008); Using the static pressure can lead to un-conservative strength calculations, even with extreme events (Barle et al., 2011);
- In fillet welds, thicker stiffeners do not always result in a more resilient connection (Roy et al., 2011);
- For multi-sided tube-to-transverse plate connections, fewer sides and sharper bend corners increase fatigue susceptibility (Roy et al., 2011);
- Fillet-welded gusseted boxes or ring-stiffened boxes do not exhibit fatigue cracks (Roy et al., 2011);
- Connections with SCF between 2 and 3 do not need inspection (infinite fatigue life) (Diekfuss 2013);
- Topography has a significant effect on wind load and consequently the fatigue life of ancillary structures. Structures in an urban area experience less wind load than in flat regions (Diekfuss 2013);
- Wind load is the only load case responsible for fatigue failure (AASHTO-LRFD 2016).

Studies identifying ancillary structures' susceptibility to fatigue failures through field testing and analytical methods made some recommendations to mitigate the conditions leading to fatigue failure. Some of these recommendations include:

- Using thicker filler welds improves the fatigue performance of the structures (Archer and Gurney 1970);
- Using airfoils increases the damping ratio which creates immunity against vortex shedding in overhead sign structures (Irwin and Peeters 1980);
- Drilling circular conduit holes causes less stress concentration than flame cutting (Chavez et al., 1997);
- U-stiffeners and ring-strengtheners reduce stress in post structures (Xiao and Yamada 2003);
- Double mast-arm structures are preferable to box truss, mono-tube, tri-chord, or single mast-arm cantilever structures for reducing fatigue failure (Li et al., 2006);
- Increasing base-plate thickness improves the fatigue life of mast arms (Anderson 2007);
- Presence of collar stiffeners in sign structures increases the fatigue life by a factor of 21 (Anderson 2007);
- Using full penetration welds allows connections to endure 20 times more cycles before failure than socket welds (Anderson 2007);
- Use thicker plates in tube-to-transverse plate connections (Roy et al., 2011);
- Using full penetration groove weld is economical for tube-to-transverse plate connections (Roy et al., 2011);
- Connections with SCF more than 4 have finite fatigue life, but instead of every 4 years can be inspected every 13-36 years (Diekfuss 2013);
- A hands-on inspection can be carried out once in the first 15 years and then every 4 years (Diekfuss 2013).

3.0 DATA COLLECTION

3.1 Overview

Two primary data types were collected for the purposes of this study. The first were historical wind measurements collected from weather stations in Cache County, Utah. The second data were the geometry and locations of traffic structures across the state of Utah, though only traffic signal structures in Cache County, Utah, were used as examples for the methodology proposed in this study.

The data processing outlined in this study was adapted from Diekfuss (2013). Data were downloaded manually from MesoWest (Horel et al., 2002) via Synoptic Labs ("Synoptic Data" n.d.), a website which curates weather data from a variety of stations (Utah Department of Transportation, National Weather Service, Utah Climate Center, etc.) into a single database, and is regularly updated as weather information is collected from various sources. The data of interest in this study were the historical wind speed/directions pairs for 31 measurement locations in Cache Valley. These locations have widely varying periods of records ranging from more than 20 years to a single month. The raw dataset contains 8,257,116 observations, though 36 of these observations were removed for having wind values exceeding the wind gust record set in 1999 for a valley location in Utah of 113 mph ("113-mph Winds Set Utah Record", Deseret News, 1999). The raw data are available in a zip folder associated with this report. Table 3.1 lists the locations of weather stations where the wind data was collected.

Table 3.1 Data Collection Locations

No.	Station ID	Station Name	Latitude	Longitude	Elevation (ft)
1	AR551	KG7EW Mendon	41.71431	-111.975	4475
2	C2247	CW2247 Weston	42.03333	-111.983	4809
3	C8633	CW8633 Richmond 1436A	41.94033	-111.813	4551
4	C8916	CW8916 Wellsville 1435	41.61583	-111.933	4665
5	C8917	CW8917 Logan 1436	41.73533	-111.855	4465
6	CAJU1	CACHE JUNCTION	41.81568	-111.98	4424
7	E1026	EW1026 Logan	41.73266	-111.839	4531
8	E2066	EW2066 Nibley	41.679	-111.873	4541
9	E3796	EW3796 Weston	42.00667	-111.918	4528
10	F2580	FW2580 Hyrum	41.638	-111.866	4652
11	FG017	River Heights	41.7254	-111.806	4669
12	ITD04	Franklin	42.01175	-111.806	4508
13	KLGU	Logan-Cache Airport	41.78652	-111.852	4446
14	LRGCC	Logan River Golf Course Climate Station	41.70564	-111.854	4475
15	MEN	MENDON	41.71	-111.98	4524
16	NLGUT	North Logan - Green Canyon	41.76553	-111.789	4875
17	QSM	Smithfield	41.84278	-111.852	4512
18	UCC04	Lewiston	41.95213	-111.869	4514
19	UCC08	Logan Golf	41.74468	-111.789	4808
20	UCC09	Drainage Farm	41.76295	-111.879	4435
21	UCC10	Evan’s Farm	41.6945	-111.833	4535
22	UCC23	Greenville Farm	41.76648	-111.811	4635
23	UCC26	LBW Exp Farm	41.66622	-111.891	4498
24	UCC27	East Fork	41.4967	-111.819	5112
25	UCC28	LBW Paradise	41.5724	-111.855	4859
26	UCC29	LBW South Fork	41.53554	-111.806	5095
27	UCC32	Clarkston	41.8957	-112.048	4940
28	UCL02	Paradise	41.54953	-111.85	5492
29	UT30	SR-30	41.779	-112.022	4990
30	UTUSU	US-89 at USU	41.73977	-111.811	4787
31	UTWEL	US-91 at MP 20 Wellsville	41.6562	-111.903	4498

3.2 Aggregation and Adjustments

The wind data were collected for use in determining the effects of wind on the traffic poles over time. Primarily, the repeated buffeting of the traffic structures by these wind loads leads to the accumulation of fatigue stresses in critical locations of the traffic structures. These stresses

could eventually lead to failure of the structures under a stress that is below their design stress limit. The above referenced wind data is used to develop a wind load history for the traffic structures, which is then used to estimate the damage which has accumulated in critical sections of the structure, allowing for an extrapolation to be made as to their continued serviceability.

Each station has a different temporal resolution of wind measurements, requiring the observations to be adjusted to a common, hourly average. Simiu and Scanlan (1996) provide a rigorous review of methods for adjusting recorded wind averages. Their review includes a discussion of the Durst curve (Vellozzi and Cohen 1970), based on the studies of Durst (1960). This curve is commonly used to convert the standard two-minute wind average (120 seconds) to a one-hour average (3600 seconds). This curve is provided in several locations, including ASCE 7-16 (ASCE 2017). Unfortunately, the full set of parameters for this curve is not provided in the accessible literature, though Simiu and Scanlan (1996) provide tabulated values for specific time intervals. The current effort uses cubic splines to approximately reconstruct the Durst curve using the tabulated values. The reconstructed curve is shown in Figure 3.1. Note that the exact conversion factor between a two-minute average wind speed s_{120} and a one-hour average s_{3600} is $\frac{s_{120}}{s_{3600}} = 1.175$. The reconstruction of this curve returns an adjustment factor of 1.178, which is only a 0.2% relative difference. This adjustment implies that the hourly wind average will be $\frac{1}{1.178} = 0.849$ times the maximum observed two-minute wind average.

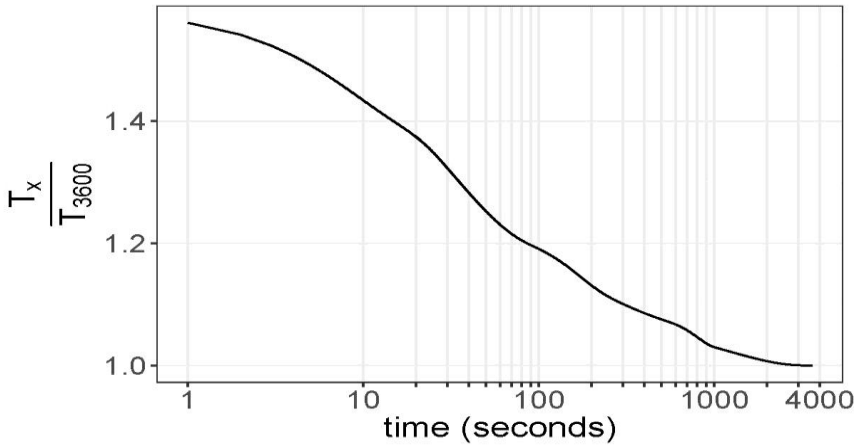

Figure 3.1 Reconstructed Durst curve which adjusts recorded wind speeds to hourly averages.

The adjustment procedure for situations with multiple observations in a single hour is illustrated by way of example. Suppose that a station contains four measurements in each hour. It is assumed that each of these measurements are two-minute wind speed averages taken at regular 15-minute intervals. These two-minute averages are converted to 15-minute averages using the Durst curve adjustment shown in Equation 3.1.

$$\frac{s_{120}}{s_{900}} = \frac{s_{120}}{s_{3600}} * \frac{s_{3600}}{s_{900}} = \frac{1.178}{1.036} = 1.137 \quad (3.1)$$

This means that the adjusted 15-minute wind speed s_{900} can be obtained from the original two-minute wind speed s_{120} as

$$s_{900_i} = \frac{s_{120_i}}{1.137} \ (i = 1, 2, 3, 4) \quad (3.2)$$

The four values s_{900_i} are then averaged together to obtain an average hourly wind speed.

In addition to adjusting/averaging the wind speeds, it is also necessary to average the wind directions. Diekfuss (2013) converted wind directions (θ), to cartesian coordinates x and y assuming a constant wind speed, averaged the x and y components, then converted the averaged x and y components back to speed (s) and direction (θ). Their approach, however, fails to give greater weight to wind directions associated with greater wind speeds. The remedy to this issue requires an adjustment to the Diekfuss (2013) approach by preserving wind speed information in the conversion to Cartesian coordinates using equation 3.3 and 3.4

$$x_i = s_i * \cos\left(\frac{\pi\theta_i}{180}\right) \quad (3.3)$$

$$y_i = s_i * \sin\left(\frac{\pi\theta_i}{180}\right). \quad (3.4)$$

The averaged components $\bar{x}$ and $\bar{y}$ can then be used to recover the average wind direction $\bar{d}$ as

$$\bar{d} = \tan^{-1}\left(\frac{\bar{y}}{\bar{x}}\right) * \frac{180}{\pi} + (180 * I_{\bar{x}<0}) + \left(360 * I_{\bar{x}>0 \ \&\bar{y}>0}\right) \quad (3.5)$$

where *I* is an indicator function (1 if true, 0 if false) that is used to adjust the returned value of the inverse tangent function based on the wind direction.

3.3 Consolidation and Filtering

This process results in 1,646,404 hourly averages of wind speeds at the 31 locations. Of these measurements, 230,564 are missing wind directions, usually because no wind was recorded during that hour. Figure 3.2 shows histograms of the frequency of observed hourly wind speeds at

each location. These histograms show the tendency for each location to occasionally have much higher wind speeds than average. Figure 3.3 shows that wind speeds differ, sometimes greatly, depending on the prevailing wind direction. In these "rose plots" the distance from the origin to the edge of the circle represents the average wind speed in that direction. While it is difficult to determine the exact average in any given wind direction in Figure 3.3, the figure illustrates the dependency between wind speed and direction for certain locations in Cache Valley. This could cause the fatigue of co-located traffic poles to vary simply based on orientation. Therefore, wind speed and direction must be considered jointly.

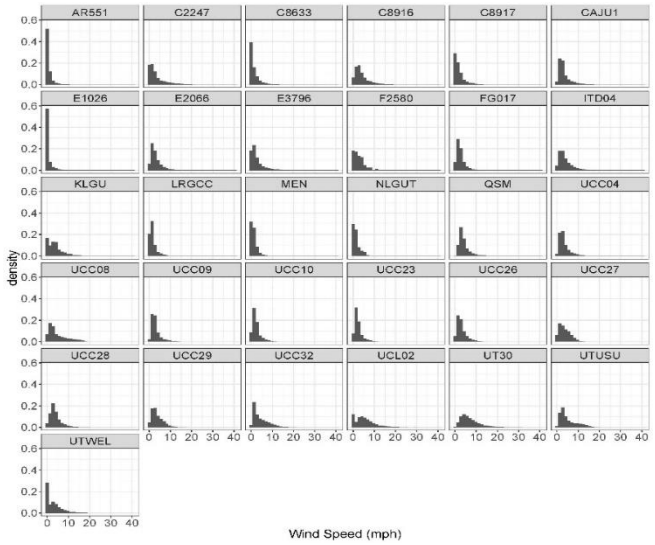

Figure 3.2 Histograms of wind speeds at each candidate station.

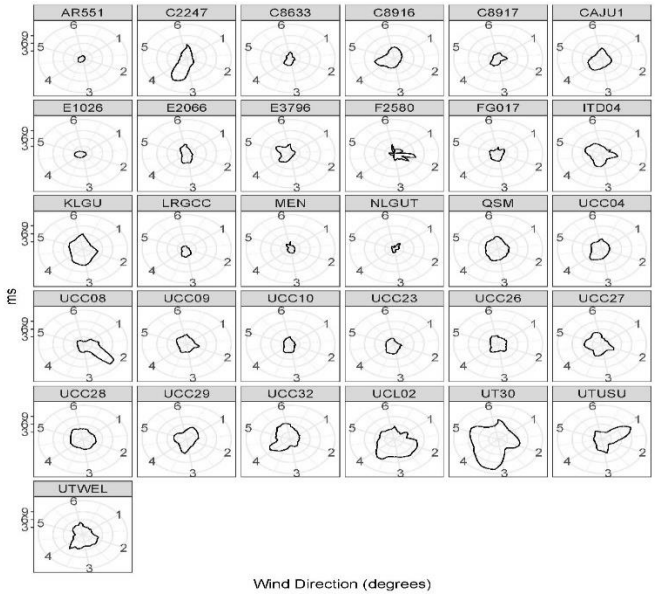

Figure 3.3 Rose plots of average wind speeds in each direction for each candidate station.

An empirical joint probability distribution of wind speeds and direction is obtained for each measurement location by binning hourly wind speeds using the eight cardinal/intercardinal directions and 0.5 mph bins for wind speed. The final bin collects all hourly average wind speeds that exceed 36 miles per hour, which only includes 15 observations in the more than 1.6 million observations. Estimating probabilities of wind speed/direction pairs are based on small sample sizes beyond 10-12 mph. However, the focus on the *long-term* effects of wind on traffic arm fatigue substantially limits the effect of any minor irregularities in extreme wind speed measurements on the resulting stress calculations.

Binned speed/direction pairs are standardized based on the total number of observations. Mathematically, this is represented as

$$\Pr(s_a < S \leq s_b \;\&\; \theta_a < \Theta \leq \theta_b) = \frac{\sum_{h=1}^{N} [I_{(sa,s_b]}(s_h) * I_{(\theta a,\theta_b]}(\theta_h)}{N} \tag{3.6}$$

where h represents one of the N hours of available records at the measurement location.

This creates a matrix S_Θ where each entry in the matrix represents the probability of observing a particular wind speed in a particular direction. The sum of the values in the matrix is the estimated probability of observing a non-zero wind speed. Figure 3.4 shows a heat map of the wind speed/direction probabilities for station UCC08 located at the mouth of Logan Canyon. Note that the sum of the matrix entries in this instance sum to 0.984 indicating that the probability of a particular hour having no measurable wind is 1.6%. The proportion of zero-valued wind measurement ranges from 0 in Smithfield to 65% at a sheltered location in downtown Logan. The median proportion of zero-valued wind measurements is 3.2%. Figure 3.5 shows a boxplot of the zero-valued wind years. Note that the lone station with greater than 50% zero-valued wind measurements was removed from consideration as the anomalously high number of zero-valued observations could not be corroborated by surrounding station locations.

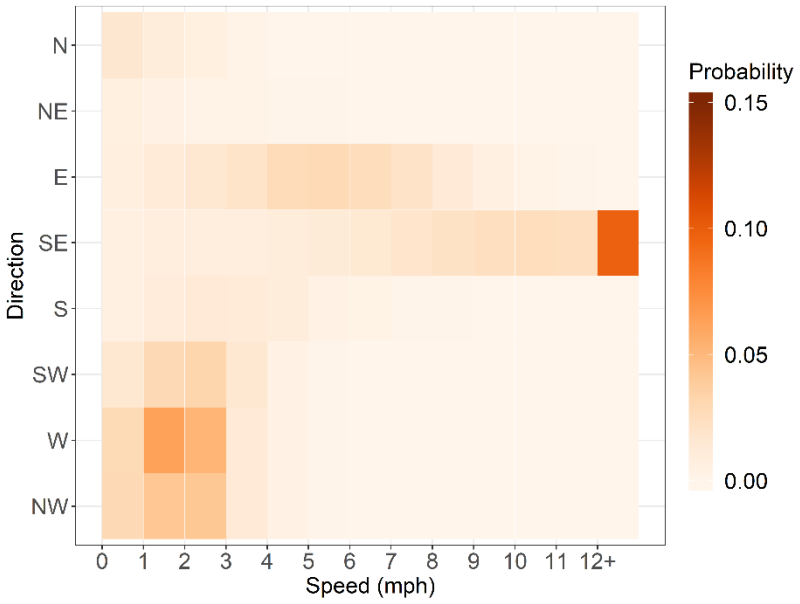

Figure 3.4 Sample heat map of the joint probability of wind speed/direction at the Logan Country Club Golf Course (41.745 N, 111.789 W).

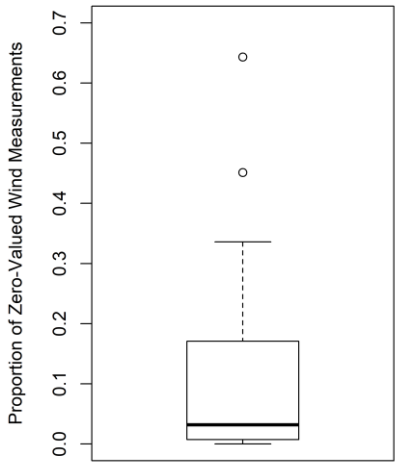

Figure 3.5 Boxplot showing the proportion of zero-valued wind measurements at the 26 qualifying measurement locations.

To ensure relatively stable estimates of the joint probability distribution, stations are required to have at least 18,000 hourly wind observations, which is slightly more than two years of hourly records. The threshold disqualifies five of the candidate measurement locations from consideration in the analysis. This threshold balances estimation accuracy (where more data is always better) with data availability. For example, a threshold larger than 18,000 hours would have

excluded the lone wind measurement station in Smithfield, UT without any nearby stations to compensate for the removal.

Figure 3.6 shows rose plots of wind speeds at qualifying measurement locations in Cache County. This figure illustrates the sharp change in wind dynamics at or near the mouth of each canyon in the valley. Traditional interpolation techniques struggle to characterize this sharp change in wind dynamics over such short distances. Unfortunately, there are no well-established methods that address this issue, and the development of such methods falls beyond the scope of this current project. In the absence of these innovations, this report follows the precedent set in Diekfuss (2013) by using inverse distance weighting to estimate the matrix of wind probabilities between measurement locations. Details regarding the interpolation process and its role in the stress cycle calculation are provided in the following chapter.

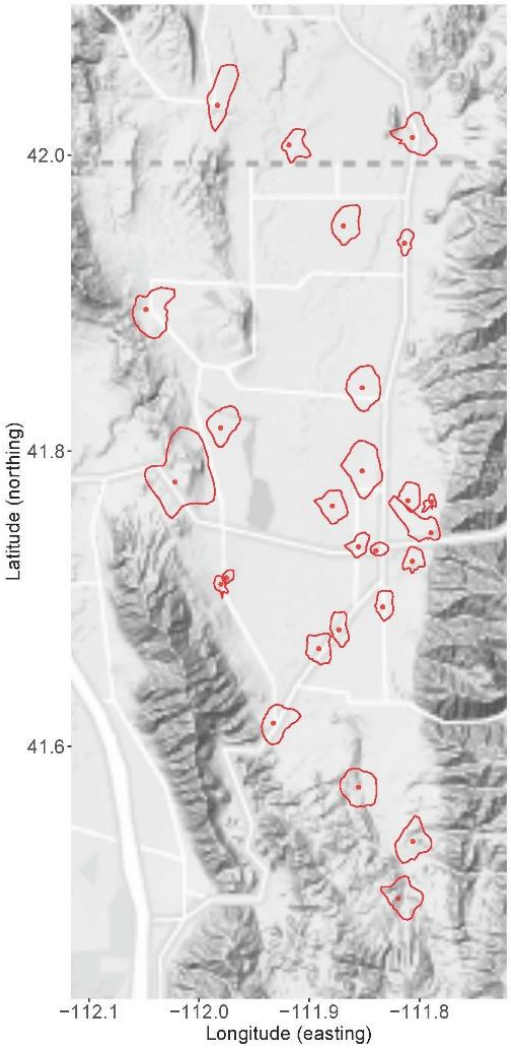

Figure 3.6 Wind rose plots for qualifying stations in Cache Valley.

3.4 Location and Geometry of Traffic Structures

Information on the location and geometry of traffic structures around the city of Logan, Utah, were collected for use in a pilot case study of the traffic structures' risk management methodology in development. Also collected were the dates of installation of these structures. These were collected from the Utah Department of Transportation (UDOT).

4.0 FATIGUE STRESS EVALUATION

4.1 Overview

Evaluation of the fatigue stress induced at critical locations of the traffic structures involves several procedures. These procedures involve the extrapolation of loading forces from the collected wind data and the internal stresses induced by these forces on the traffic structure. Beyond the internal stresses, fatigue damage accumulated over time is computed using Miner's rule of damage accumulation using the number of cycles the winds are expected to induce upon the traffic structure.

4.2 Wind Stresses

4.2.1 Wind Speed Correction

Wind speeds are initially corrected for height, to allow for changes in wind speed with respect to height differences between the wind speed measurements and the heights of critical sections of the traffic structure. This correction for height is carried out using Equation 4.1.

$$U(Z) = U_1 \left(\frac{Z}{Z_1}\right)^{\alpha} \quad \text{(mph)} \tag{4.1}$$

Where: U(Z) is the wind speed at height Z, U_1 is the reference mean wind speed at reference height Z_1.

An assumption made in correcting the wind speeds for height is that all wind data is collected at a standard height of 33 ft (10 m) above the ground surface. Although recognizably, this is not the case as some of the data collection stations are known to not be placed at this height. However, data on the height of all the stations is not available and as such, this assumption is made.

Wind speeds can be expected to occur at a range of angles between 0^o and 360^o. On the other hand, the traffic structure is installed at a specific angle. As such, the wind strikes the traffic structure at different angles, creating varying pressures. In analyzing these wind pressures, it is necessary to correct the measured wind speeds for the direction with respect to the position of the traffic structure. Diekfuss (2013) developed a set of equations for correcting wind speed with

respect to direction using the cosines of angles between the wind direction and traffic structures as shown in Equation 4.2 below.

$$U_{adj} = U_w * \cos((90 - \theta) + D_w) \quad \text{for } 0^o < D_w \leq \theta$$

$$U_{adj} = U_w * \cos((90 + \theta) - D_w) \quad \text{for } \theta < D_w \leq (90+\theta)$$

$$U_{adj} = U_w * \cos(D_w - (90 + \theta)) \quad \text{for } (90+\theta) < D_w \leq (180+\theta) \qquad (4.2)$$

$$U_{adj} = U_w * \cos((270 + \theta) - D_w) \quad \text{for } (180+\theta) < D_w \leq (270+\theta)$$

$$U_{adj} = U_w * \cos(D_w - (270 + \theta)) \quad \text{for } D_w > (270+\theta)$$

where U_w is denotes the original wind speed, U_{adj} is the adjusted wind speed, D_w is the measured wind direction, and θ is the direction of traffic structure.

The process of binning wind speed/direction pairs is necessary to generate reasonable estimates of wind speed/direction profiles at traffic structure locations using nearby weather stations. However, the binning process makes it difficult to directly apply the direction adjustments described in Equation 4.2. As such, the simplifying assumption is made that all traffic structures in Cache County have mast arms oriented in the due east/west, or due north/south direction. Structures with mast arms oriented in the north/south direction are assumed to be constantly subject to the full force of winds blowing in the east/west direction, while subject to the full force of winds blowing in the northeast/southwest or northwest/southeast directions for only half the time. Similar assumptions are made for structures with mast arms oriented in the north/south direction.

4.2.2 Wind Pressures

These wind speeds are converted to wind pressures using the AASHTO expression shown in Equation 4.3 (Diekfuss 2013).

$$P(t) = \frac{1}{2}\rho . C_d . U^2(t) \qquad (4.3)$$

where P is the wind pressure, ρ is the density of air (kip.s^2/in^4), C_d is the drag coefficient, and U is the wind speed (in/s).

4.2.3 Wind Stresses

The wind pressures are converted to wind forces acting at different locations of the traffic structure including the mast arm, attachments, and luminaire, depending on the structure's particular geometry as shown in Equations 4.4 to 4.6.

$$F_{mastarm} = \frac{1}{2} * Dia_{mastarm} * Lt_{mastarm} * P(mastarm) \quad (4.4)$$

$$F_{sign} = Area_{sign} * P(sign) \quad (4.5)$$

$$F_{pole} = \frac{1}{2} * Dia_{pole} * Lt_{pole} * P(pole) \quad (4.6)$$

where F is the wind force acting on different locations, Dia is the diameter of the location in question (in), and Lt is the length of the location (in).

Next, position vectors for each of the computed equivalent wind forces are defined and the moment vector for each of the components is computed by cross multiplying the position vector with the force vector.

$$M = \bar{r} * \bar{F} \quad (4.7)$$

where $\bar{r}$ is the position vector and $\bar{F}$ is the force vector.

Two critical locations for fatigue stresses have been identified. These are the mast-arm-to-baseplate connection and the pole-to-baseplate connection. Fatigue damage is monitored in this study at these two locations for all traffic signal structures.

In computing the moments at the mast arm baseplate connection, only the wind forces acting on the mast arm and its attachments are used and their position vectors are the positions of each component from the mast arm base.

Moments at the pole-to-baseplate connection are computed for all components of the traffic signal structure, with their respective position vectors ($\bar{r}$) being the position of each location of interest from the baseplate, and the forces acting on them from the winds computed as shown in Equations 4.4 to 4.6.

Summing together the different components of the moment vectors and taking the square root of the sum of squares of the resulting vector gives the resultant moment (M_{res}) at the base of the pole.

The bending stress (σ) from this resulting moment is then computed as shown in Equations 4.8 to 4.10 below.

$$\sigma = \frac{M_{res} * y}{I} \tag{4.8}$$

$$I = \frac{\pi}{4} * \left(D_{out}^4 - D_{in}^4\right) \tag{4.9}$$

$$y = \frac{D_{out}}{2} \tag{4.10}$$

where σ is the bending stress (ksi), M_{res} is the resultant moment from the wind forces, y is the maximum distance to the neutral axis of the cross-section (in), I is the moment of inertia of the cross section (in^4), D_{out} and D_{in} are the external and internal diameters of the cross section respectively (in).

These bending stresses from the wind loads are then used in computing the fatigue damage expected to occur for each cycle of loading. Accumulation of this damage over time could lead to failure of the structure. The procedure for computing the accumulated damage is described in the next section.

4.2.4 Fatigue Damage Computation

This study utilized Palmgren-Miner's rule for damage accumulation (Miner 1945) to compute the damage from cyclic wind loads to the pole and baseplate connection. This rule postulates that the damage occurring for each cyclic load is a fraction of the number of cycles the material in question has endured at a particular stress to the number of cycles the material can endure at that stress range before failing. A summation of this damage fraction for the different stress ranges gives the cumulative fatigue damage for the material. This total cumulative damage is computed as shown in Equation 4.11 (Miner 1945).

$$D = \sum_{i=1}^{k} \frac{N_{cyc,i}}{N_{f,i}} \tag{4.11}$$

where D is the damage sustained by the traffic structure, k is the total length of the wind history data, $N_{cyc,i}$ is the number of cycles endured by the material at stress range i, and $N_{f,i}$ is the number of cycles to failure at a particular stress range i.

The number of cycles endured at a particular stress range (N_{cyc}) is obtained from AASHTO specifications, which gives the expected number of cycles for different stress ranges (AASHTO-LRFD 2016). Table 4.1shows this data.

Table 4.1 Number of Cycles for Different Stress Ranges

Mean Wind Speed	Number of Cycles per Day (N_{day})
$V_{mean} \leq 9$mph	9,500
9 mph < $V_{mean} \leq 11$ mph	15,000
$V_{mean} > 11$ mph	23,000
Vortex Shedding Mitigated	7,000

The number of cycles to failure for a particular material at a specific stress range is computed as shown in Equation 4.12.

$$N_f = N_2 * \left(\frac{S_i}{S_2}\right)^{\frac{1}{b}} \tag{4.12}$$

where N_f is the number of cycles to failure at a particular stress, S_i is the stress induced by a particular wind speed, N_2 is the number of cycles to failure at stress level S_2, and b is the slope of the S-N curve for the material.

The slope of the S-N curve for the material is computed using Basquin's relationship (Basquin 1910) as shown in Equation 4.13.

$$b = \frac{-(\log_{10} S_1 - \log_{10} S_2)}{(\log_{10} N_2 - \log_{10} N_1)} \tag{4.13}$$

where b is slope of the S-N curve, S_1 and S_2 are stresses along the curve, and N_1 and N_2 are the number of cycles to failure at those stresses.

For this study, all welded connections are assumed to be fatigue category E as per AASHTO regulations, and the material is assumed to be steel. Thus, the material S-N curve data used in estimating the fatigue behavior are as shown in Figure 4.1 below (AASHTO-LRFD 2016).

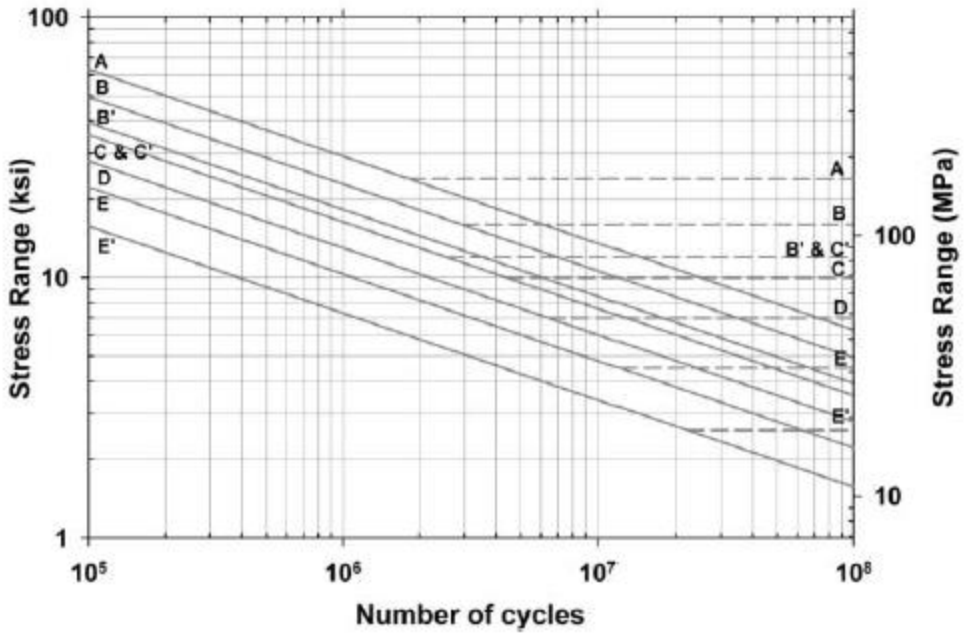

Figure 4.1 Stress Range vs Number of Cycles to Failure

4.3 Damage Accumulation Due to Fatigue Stress

The methodology described above for determining the fatigue life in traffic structures utilizes an intricate set of procedures which are dependent on specific geometrical dimensions of the structure. However, most installed traffic structures fall within a finite combination of geometric configurations. As such, stress calculations were only performed for a finite combination of lengths and diameters of mast arms and traffic poles with and without affixed luminaires. Fatigue stresses were computed for these specific geometries for wind speeds ranging from 0 to 36.5 mph. Stresses for the wind speed history at a particular location and geometry can then be extracted and used in computing the accumulated damage for a particular traffic structure of interest. The assumptions made for the analyses, the design of the fatigue life monitoring tool, as well as some results are presented in this section.

4.3.1 Analysis Parameters

The geometric dimensions of the pole were obtained from UDOT drawings. Figure 4.2 shows a schematic of the traffic pole obtained from UDOT specification SL01A (“Standard Specifications & Standard Drawings" | UDOT n.d.).

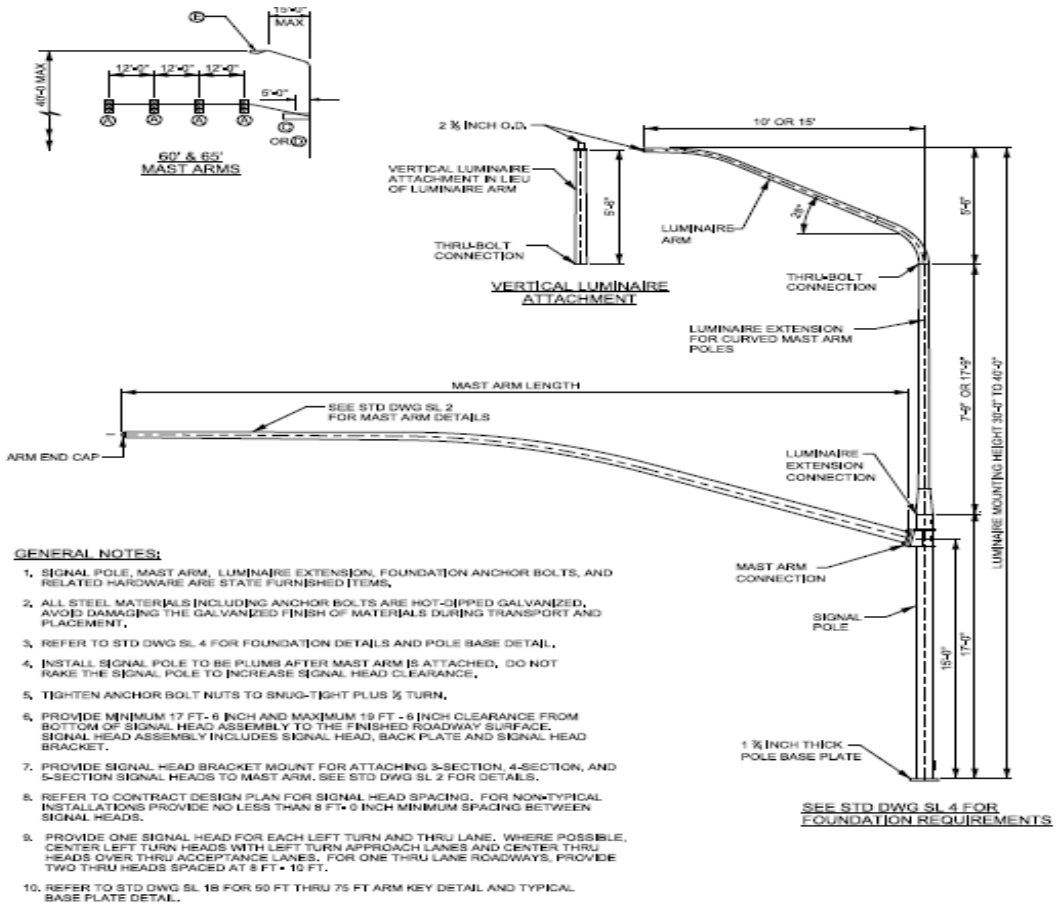

Figure 4.2 Standard traffic pole from UDOT specifications

In computing wind stresses, some simplifying assumptions were made for geometric configurations, material properties, and in-service state of the structure:

The connections are assumed to be in perfect shape with the welded joints not having any imperfections or cracks. All the traffic structures are assumed to be steel and the pole-to-baseplate connections to be category E. As such, the stress to number of cycles to failure (S-N) curve for this scenario is used in estimating the fatigue life for all the traffic structures.

Some geometric dimensions are assumed to be the same for all the traffic structures. These include the diameter and height of the poles and luminaire poles, the thickness of the poles, and the taper for poles and mast arms. Different permutations for the other dimensions were used and the presence or absence of a luminaire pole above the traffic pole is also considered. Table 4.2 below shows the geometric dimensions used.

Table 4.2 Design Parameters Used in the Analysis

Design Parameters		
Parameter	Value	Unit
Length of pole	17	ft.
Diameter of pole bottom	16	in.
Taper of pole	0.12	in. per ft.
Thickness of pole	0.1793	in.
Height of mast arm connection	15	ft.
Angle of mast arm	12	degrees
Length of mast arm	25-65	ft.
Taper of mast arm	0.12	in. per ft.
Diameter of mast arm base	7.75-12	in.
Length of luminaire pole	17.75	ft.
Taper of luminaire pole	0.12	in. per ft.
Angle of luminaire	28	degrees
Attachments		
Area of traffic light	8.7	ft^2
Area of turn lights	11.1	ft^2
Area of street label	20	ft^2
Area of light fixture	3	ft^2

Some assumptions are also made regarding the number of attachments on the mast arms. Mast arms between 25 and 35 feet in length are assumed to only have two light fixtures and a street label attached, those between 40 and 55 feet are assumed to carry two light fixtures and a separate turn signal, while those over 55 feet are assumed to carry two turn signals in addition to two light fixtures.

The wind fatigue stress analysis was carried out using these assumptions and the previously described methodology, and a monitoring tool developed off these analyses was developed to allow for remote monitoring of the fatigue life and damage state of the traffic structures. The developed app and its features are described in the next section.

4.3.2 Traffic Structures' Monitoring App

The app associated with this report allows users to interactively explore the expected fatigue life of traffic structures in Cache County, Utah. The app was developed using R 4.0.3 statistical software (Team and DC 2019) with the help of the gstat (Benedikt et al., 2016; Pebesma

2004), leaflet (Cheng et al., 2018), shiny (Chang et al., 2019), sp (Bivand et al., 2013; Pebesma and Bivand 2005), and tidyverse (Wickham et al., 2019) ancillary software packages. Instructions for running an offline version of this app are provided in a folder of necessary files for running the app using Rstudio ("RStudio | Open source & professional software for data science teams - RStudio" n.d.), which is a user-friendly interface to the R programming language.

Figure 4.3 shows a screen shot of the app dashboard. Users are first prompted to select a traffic structure location, which is indicated by the blue circles on the included map of Cache County. Note that the map allows users to scroll and zoom to obtain better discrimination between traffic structure locations in downtown Logan or for locations in Cache County not seen in the current view. The selected location is represented by a red circle that appears when the user selects a location.

Once a location has been selected, the user is presented with two figures and a table. The first visual (panning left to right) are histograms of the stress induced by hourly wind speeds for traffic structures with mast arms oriented in the east/west and north/south directions. The histogram visual can be adjusted using the "Bin Width" slider bar. This slider determines the size of the histogram bins and does not change the time to failure estimates provided in the table located in the center of the dashboard. Note that structures with mast arms oriented in the east/west direction are subject to stresses induced by north/south winds and vice versa, which is why the two histograms are not identical. The time to failure estimates for both the mast arm and the base pole change in response to user-defined inputs in the "Stress Cycle Inputs" column, where the user is given a discrete set of mast arm lengths and diameters to choose from. Users are also given an option to include or exclude traffic lights on the mast arm and can also select the stress threshold above which stress cycles are assumed to cause damage.

The final visual that appears is a heat map showing the estimated joint probabilities of wind speed and direction. Darker squares indicate a greater likelihood of observing a particular wind speed/direction pair. (An example of this visual was previously provided in Figure 3.4.) The user has the option to change the appearance of this plot with the "wind speed inputs sliders" provided on the far-left side of the dashboard. The "Bins (mph)" and "Directions" sliders change the bin sizes in the heat map but only the "Directions" slider has any influence on the time to failure estimates. All wind speeds exceeding 12 mph are reflected in the far-right bins of the heat map. The choice to stop bin separation at 12 mph ensures that the most typical wind speed/direction

combinations can be effectively visualized, as it is too difficult to discriminate between the small probabilities that occur in bins with hourly wind speeds exceeding 12 mph. The "show expected hourly wind frequencies" checkbox populates each square of the heat map with the number of hours that a particular wind speed/direction pair is to be expected during a given year.

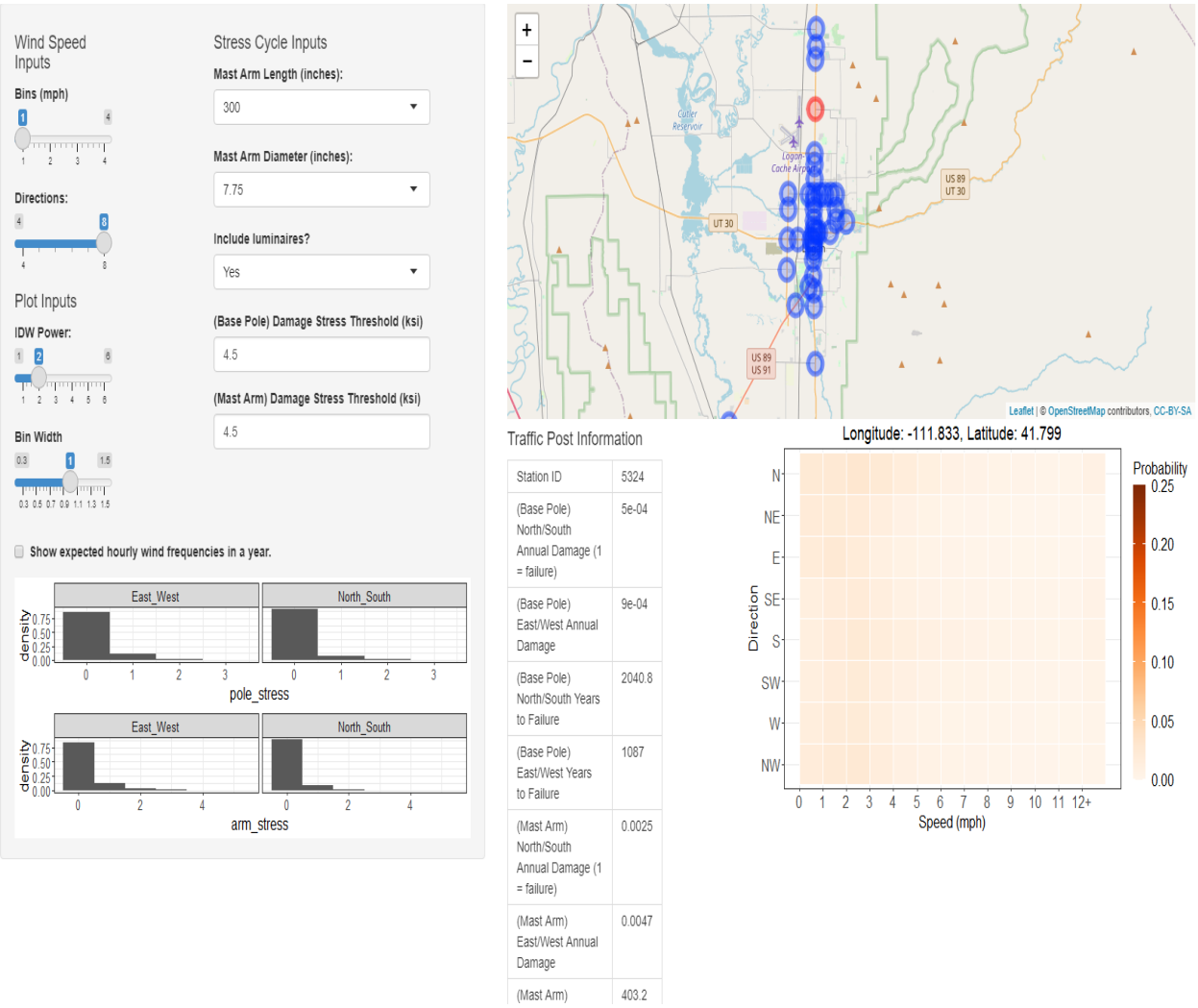

Figure 4.3 Screenshot of the app dashboard for determining estimated years to failure for traffic structures in Cache County, Utah.

Recall that the wind speed/direction matrix of probabilities at a traffic structure location is estimated using a weighted average of the observed speed/direction probabilities at nearby weather stations. Weights are assigned using the inverse of the geographical distance $D(\boldsymbol{x}^*, \boldsymbol{x}_\alpha)$ between a traffic pole location $\boldsymbol{x}^*$ and the surrounding weather stations $\boldsymbol{x}_\alpha$ (Shepard 1968). This is represented mathematically as:

$$S_\Theta(\boldsymbol{x}^*) = \frac{\sum_{\alpha=1}^{N} w(\boldsymbol{x}_\alpha) S_\Theta(\boldsymbol{x}_\alpha)}{\sum_{\alpha=1}^{N} w(\boldsymbol{x}_\alpha)} \tag{4.14}$$

where

$$w(\boldsymbol{x}_\alpha) = \frac{1}{D(\boldsymbol{x}^*, \boldsymbol{x}_\alpha)^p}.$$

The parameter p controls the influence of nearby stations as compared to far-away stations. Larger values of p give greater influence to nearby stations, but may be overly sensitive to station-specific anomalies. Smaller values of p are less sensitive to station-specific anomalies, but risk losing over smoothing known geographic differences in wind patterns. The user has the option to select this parameter with the "IDW power" slider, though the default value of two is most used in practice. The location-specific wind speed/direction matrix is used to determine the expected number of hours that the traffic pole will be subject to each wind speed/direction combination. The user has the option to change the number of wind directions, which changes the probability matrix. On the other hand, any changes to the wind speed bins are for visual purposes only and do not change the wind speed/direction bins for the fatigue calculations. Fatigue cycles are calculated using the expected number of cycles in a single hour for a given wind speed, multiplied by the expected number of hours that the wind will blow at that speed in a relevant direction.

The key advantage of the app is that it allows the user to experiment with different interpolation schemes, stress thresholds, and traffic structure geometries in real time. Doing so allows the user to get a sense of the *patterns* in the estimated stresses induced by wind upon traffic structures, which may be more important than the estimated values themselves.

4.3.3 Fatigue Life of Selected Traffic Structures

In testing the utility of the developed tool, the fatigue service lives of some traffic structures around the city of Logan were determined. This was done by selecting the location of the particular traffic structure of interest from the map in the application and selecting some of its known geometric dimensions such as the mast arm length and the mast arm diameter. The application then computes the damage incurred by this structure using wind data for this location and outputs the expected fatigue life of the structure. Tables 4.3 and 4.4 show the results for the different traffic structures tested.

Table 4.3 Fatigue Life Estimates for Pole-to-Baseplate Connection on Traffic Poles around Logan, Utah

				N-S Bound		E-W Bound	
	Location	Install Date	Mast Arm Length	Fatigue Life (years)	Time Left in Service (years)	Fatigue Life (years)	Time Left in Service (years)
1	1800 N & Main Logan	1993	EB 30' NB 50'	242.7	214.7	1724.1	1696.1
2	2200 N & Main Logan	1999	EB 35' SB 55'	121.2	99.2	719.4	697.4
3	Hyde Park US 91 Hyde Park	1997	EB 40' SB 50'	113.4	89.4	135.7	111.7
4	600 S US 91 Smithfield	2005	NB 40' EB 40'	471.7	455.7	192.7	176.7
5	100 N US 91 Smithfield	2008	NB 45' EB 40'	431	418	214.1	201.1
6	Richmond US 91	2006	WB 40' SB 60'	184.5	169.5	826.4	811.4
7	1400 N & Main Logan	2002	NB 60' EB 50'	75.4	56.4	171.2	152.2
8	700 N & Main Logan	1978	NB 40' EB 25'	1162.8	1119.8	5555.6	5512.6
9	500 N & Main Logan	1981	WB 25' SB 55'	282.5	242.5	6250	6210
10	400 N & Main Logan	1999	NB 65' WB 45'	78.1	56.1	469.5	447.5
11	400 N & 200 E Logan	1980	NB 40' WB 40'	1333.3	1292.3	757.6	716.6
12	200 N & Main Logan	1981	SB 55' WB 40'	325.7	285.7	862.1	822.1
13	300 S & Main Logan	1982	SB 40' WB 30'	1666.7	1627.7	5000	4961
14	1400 N & 10th West Logan	2011	NB 55' WB 60'	186.9	176.9	42.8	32.8
15	200 N & 1000 W Logan	2011	WB 60' SB 55'	1515.2	1505.2	375.9	365.9

Table 4.4 Fatigue Life Estimates for Mast-Arm-to-Baseplate Connection on Traffic Poles around Logan, Utah

				N-S Bound		E-W Bound	
	Location	Install Date	Mast Arm Length	Fatigue Life (years)	Time Left in Service (years)	Fatigue Life (years)	Time Left in Service (years)
1	1800 N & Main Logan	1993	EB 30' NB 50'	173	145	458.7	430.7
2	2200 N & Main Logan	1999	EB 35' SB 55'	119.2	97.2	229.9	207.9
3	Hyde Park US 91 Hyde Park	1997	EB 40' SB 50'	82.8	58.8	49	25
4	600 S US 91 Smithfield	2005	NB 40' EB 40'	160.5	144.5	67.4	51.4
5	100 N US 91 Smithfield	2008	NB 45' EB 40'	212.8	199.8	73	60
6	Richmond US 91	2006	WB 40' SB 60'	225.2	210.2	283.3	268.3
7	1400 N & Main Logan	2002	NB 60' EB 50'	92.4	73.4	122.7	103.7
8	700 N & Main Logan	1978	NB 40' EB 25'	302.1	259.1	1785.7	1742.7
9	500 N & Main Logan	1981	WB 25' SB 55'	277.8	237.8	2040.8	2000.8
10	400 N & Main Logan	1999	NB 65' WB 45'	106.7	84.7	215.5	193.5
11	400 N & 200 E Logan	1980	NB 40' WB 40'	313.5	272.5	211.4	170.4
12	200 N & Main Logan	1981	SB 55' WB 40'	320.5	280.5	251.3	211.3
13	300 S & Main Logan	1982	SB 40' WB 30'	269.5	230.5	1315.8	1276.8
14	1400 N & 10th West Logan	2011	NB 55' WB 60'	183.8	173.8	51.9	41.9
15	200 N & 1000 W Logan	2011	WB 60' SB 55'	1492.5	1482.5	471.7	461.7

From the results, it can be opined that the traffic structures are in relatively good shape and not likely to fail from cyclic wind loads. The eastbound traffic signal mast arm on US 91 in Hyde Park has the lowest fatigue service life among the mast arm connections surveyed. The pole-to-baseplate connection of the westbound traffic light structure at the junction of 1400 N and 10th W has the lowest fatigue life of 42.8 years, due to a combination of high winds at the location and size of the mast arm. Most of the traffic structures have infinite life with regard to fatigue (structures with over 50 years expected fatigue lives are considered to have infinite lives). However, this analysis does not consider wind gusts from passing vehicles nor the possibility of intermittent extreme wind loads. Also, not considered is the possibility of flaws in the welds at the welded connections. In addition, some of the geometric configurations are assumed to be identical for all of these structures. These considerations could have a telling impact on the fatigue lives of these structures.

4.4 Summary

This section gave an overview of the process used in estimating fatigue damage to traffic signal structures from historical wind data. The presented process is then compiled into a remote monitoring tool, designed to give personnel an overview of the health of these structures, helping them in making informed decisions about the structures.

5.0 CONCLUSIONS

5.1 Summary

This study set out to develop a plan to improve the monitoring and tracking of the structural health of traffic signal structures under cyclic wind loads around the state to reduce incidences of failure. To achieve this aim, a review of literature on the performance of these slender structures under wind loads and the analysis of this performance was carried out. From this review, the pole-to-baseplate and the mast-arm-to-baseplate connections were identified as critical to the performance of the structure under this type of loading and selected for further scrutiny. Also, a procedure for estimating the fatigue damage to the structures over time was outlined that utilized historical wind speed/direction measurements to estimate the fatigue stresses, accumulated damage, and estimated fatigue life of traffic structures. Several necessary generalizing assumptions include using a limited number of geometric configurations, assuming perfect welds in the connections, and not considering the effect of wind gusts from passing vehicles on the fatigue lives of these structures. As such, the greatest value in the tool in its current form is a knowledge of the relative fatigue damage that has occurred on a traffic structure compared to the other traffic structures.

5.2 Findings

Some of the findings from this study are as follows:

- Wind speeds vary widely across the different stations used in collecting data. While some of these variations can be attributed to differences in topography, some might point to issues with the data-gathering instrumentation which would need recalibration or repair.

- Wind stresses do not inherently pose a great threat to the traffic structures. This can be seen from some example applications of the fatigue damage estimation using traffic light structures around the city of Logan. Using the wind speed data from stations around the city, the fatigue lives of these structures were estimated and

could range anywhere from around 42 years to over 5500 years. However, this does not consider other wind sources such as gusts from passing vehicles which may have a telling effect on the fatigue lives of these structures and accelerate damage. Also, these values are obtained using some assumptions including that the traffic structures under consideration are all in a perfect state of repair and the pole-to-baseplate welded connections do not have any flaws in the welds. Studies have shown that this may not commonly be the case as welded connections regularly have imperceptible flaws which may precipitate damage and accelerate the estimated failure timeline.

- There is a need for a comprehensive database of all the traffic structures around the state, including their geometrical configurations and installation dates. This will help reduce the need for making some of the simplifying assumptions made in developing the monitoring tool.

- The monitoring tool developed offers a handy solution for monitoring and tracking damage to traffic structures from wind forces over time. This tool, if deployed and utilized properly, will allow operators to gain a utilitarian view into the in-service state of these structures, helping them make informed decisions about these structures.

5.3 Limitations and Challenges

There are some limitations to the applicability of the currently developed tool. At present, this tool only contains wind speed data for the Cache Valley region and as such, can only be applied to traffic structures in this area. Also, some of the simplifying assumptions made might limit the applicability of the tool to certain structures. These include assuming the traffic poles are tubular, thus the results cannot be said to accurately represent poles of other geometrical shapes. Also, a single standard height is used for all traffic structures. As a result, any traffic structure not meeting these assumptions may not be accurately analyzed by the tool. These assumptions were made as UDOT primarily uses tubular steel for its traffic signal structures and also due to a dearth of information about the traffic structures around the valley.

6.0 RECOMMENDATIONS AND IMPLEMENTATION

6.1 Recommendations

This report details the development of a monitoring tool which estimates fatigue damage to traffic structures from wind loads over time. Some recommendations emanating from this study include;

1. The scope of the monitoring tool should be expanded to include other locations around the state.

2. The different types of traffic pole structures currently in use within the state need to be documented and used to expand the scope of the tool developed for monitoring fatigue damage.

3. Some assumptions regarding the geometry and condition of the traffic structures were made in designing the monitoring tool. As such, it is best utilized as an informative tool, to help users identify at-risk traffic structures, before better diagnostic tools are used to determine the state of the structures.

4. Validation of the monitoring process needs to be carried out by instrumenting some traffic structures and collecting the stress data for comparison with the information provided by the monitoring tool. This should be done prior to deploying the tool for use.

REFERENCES

"113-mph winds set Utah record - Deseret News." (n.d.). <https://www.deseret.com/1999/4/24/19441867/113-mph-winds-set-utah-record> (Jan. 13, 2021).

AASHTO-LRFD. (2016). *LRFD Specifications for Structural Supports for Highway Signs, Luminaries, and Traffic Signals*. *American Association of State Highway and Transportation Officials (AASHTO), Washington, DC*, American Association of State Highway and Transportation Officials (AASHTO), Washington, DC.

Albert, M. N. (2006). "Field testing of cantilevered traffic signal structures under truck-induced gust loads." University of Texas at Austin.

Alexander, L. A., and Wood, J. (2009). "A study of the low-cycle fatigue failure of a galvanised steel lighting column." *Engineering Failure Analysis*, Elsevier, 16(7), 2153–2162.

An, Y.-K., Kim, J. M., and Sohn, H. (2014). "Laser lock-in thermography for detection of surface-breaking fatigue cracks on uncoated steel structures." *Ndt & E International*, Elsevier, 65, 54–63.

Anderson, T. H. (2007). "Fatigue life investigation of traffic signal mast-arm connection details." University of Texas at Austin.

Archer, G. L., and Gurney, T. R. (1970). "Fatigue strength of mild steel fillet welded tube to plate joints." *METAL CONSTR BRIT WELD J*, 2(5), 207–210.

ASCE. (2017). *Minimum design loads and associated criteria for buildings and other structures*. American society of civil engineers.

Baird, R. C. (1955). "Wind-Induced Vibration of a Pipe-Line Suspension Bridge, and Its Cure." *TRANS. ASME*, 77, 797–804.

Barle, J., Grubisic, V., and Vlak, F. (2011). "Failure analysis of the highway sign structure and the design improvement." *Engineering failure analysis*, Elsevier, 18(3), 1076–1084.

Basquin, O. H. (1910). "The exponential law of endurance tests." *Proc Am Soc Test Mater*, 625–630.

Benedikt, G., Pebesma, E., and Heuvelink, G. (2016). "Spatio-temporal interpolation using gstat." *The R Journal*, 8(1), 204–218.

Bivand, R. S., Pebesma, E., and Gómez-Rubio, V. (2013). *Applied Spatial Data Analysis with R*.

Springer Science & Business Media.

Cali, P. M., and Covert, E. E. (2000). “Experimental measurements of the loads induced on an overhead highway sign structure by vehicle-induced gusts.” *Journal of Wind Engineering and Industrial Aerodynamics*, Elsevier, 84(1), 87–100.

Caracoglia, L., and Jones, N. (2004). *Analysis of light pole failures in Illinois. Final report*. *Civil Engineering Studies, Structural Research Series*, Urbana Champaign.

Chang, W., Cheng, J., Allaire, J. J., Xie, Y., and McPherson, J. (2019). “shiny: Web Application Framework for R. R package version 1.2. 0 (2018).”

Chavez, J. W., Gilani, A. S., and Whittaker, A. S. (1997). *Fatigue-Life Evaluation of Changeable Message Sign Structures, Volume 2-Retrofitted Structures*. Report No. UCB/EERC-97.

Chen, G., Barker, M. G., Dharani, L. R., and Ramsay, C. W. (2003). *Signal mast arm fatigue failure investigation*. University of Missouri-Columbia; University of Missouri-Rolla, Jefferson City.

Cheng, J., Karambelkar, B., and Xie, Y. (2018). “Leaflet: Create interactive web maps with the javascript’leaflet’library.” *R package version*.

Christenson, R. E., and Hoque, S. (2011). “Reducing fatigue in wind-excited support structures of traffic signals with innovative vibration absorber.” *Transportation research record*, SAGE Publications Sage CA: Los Angeles, CA, 2251(1), 16–23.

Connor, R. J. (2012). *Fatigue loading and design methodology for high-mast lighting towers*. Transportation Research Board.

Cook, R. A., Bloomquist, D., Agosta, A. M., and Taylor, K. F. (1996). *Wind load data for variable message signs*. *Florida Department of Transportation, Final Project Report-State Study*.

Cook, R. A., Bloomquist, D., Richard, D. S., and Kalajian, M. A. (2001). “Damping of cantilevered traffic signal structures.” *Journal of Structural Engineering*, American Society of Civil Engineers, 127(12), 1476–1483.

Cook, S. J., Till, R. D., and Pearson, L. (2000). “Fatigue cracking of horizontal gusset plates at arm-to-pole connection of cantilever sign structures.” *Structural Materials Technology IV-An NDT ConferenceNew York State Department of Transportation; New Jersey Department of Transportation; and Federal Highway Administration.*

Creamer, B. M., Frank, K. H., and Klingner, R. E. (1979). *Fatigue loading of cantilever sign*

structures from truck wind gusts. Austin.

DeSantis, P. V, and Haig, P. E. (1996). "Unanticipated loading causes highway sign failure." *Proceedings of ANSYS Convention*, 3–98.

Dexter, R. J., and Johns, K. W. (1998). *Fatigue-related wind loads on highway support structures: Advanced technology for large structural systems*. *Advanced technology for structural systems (ATLSS), report*.

Diekfuss, J. A. (2013). "Reliability-based fatigue assessment of mast-arm sign support structures." Marquette.

Durst, C. S. (1960). "Wind speeds over short periods of time." *Meteor. Mag*, 89(1056), 181–187.

Edwards, J. A., and Bingham, W. L. (1984). *Deflection criteria for wind induced vibrations in cantilever highway sign structures*. Raleigh.

Fouad, F. H., Davidson, J. S., Delatte, N., Calvert, E. A., CHEN, S. E., Nunez, E., and Abdalla, R. (2003). *STRUCTURAL SUPPORTS FOR HIGHWAY SIGNS, LUMINAIRES, AND TRAFFIC SIGNALS*. Birmingham.

Garlich, M. J., and Thorkildsen, E. T. (2005). *Guidelines for the installation, inspection, maintenance and repair of structural supports for highway signs, luminaires, and traffic signals*. United States. Federal Highway Administration.

Garrido, I., Lagüela, S., and Arias, P. (2018). "Infrared Thermography's Application to Infrastructure Inspections." *Infrastructures*, Multidisciplinary Digital Publishing Institute, 3(3), 35.

Gilani, A. S., Chavez, J. W., and Whittaker, A. S. (1997). *FATIGUE LIFE EVALUATION OF CHANGEABLE MESSAGE SIGN STRUCTURES. VOLUME 1, AS-BUILT SPECIMENS*. Berkeley.

Gilani, A., and Whittaker, A. (2000a). "Fatigue-life evaluation of steel post structures. I: Background and analysis." *Journal of Structural Engineering*, American Society of Civil Engineers, 126(3), 322–330.

Gilani, A., and Whittaker, A. (2000b). "Fatigue-life evaluation of steel post structures. II: Experimentation." *Journal of Structural Engineering*, American Society of Civil Engineers, 126(3), 331–340.

Ginal, S. (2003). "Fatigue performance of full-span sign support structures considering truck-induced gust and natural wind pressures." Marquette University.

Hamilton III, H. R., Riggs, G. S., and Puckett, J. A. (2000). “Increased damping in cantilevered traffic signal structures.” *Journal of Structural Engineering*, American Society of Civil Engineers, 126(4), 530–537.

Hartle, R. A., Amrhein, W. J., Wilson III, K. E., Baughman, D. R., and Tkacs, J. J. (1995). *Bridge Inspector’s Training Manual/90*.

Horel, J., Splitt, M., Dunn, L., Pechmann, J., White, B., Ciliberti, C., Lazarus, S., Slemmer, J., Zaff, D., and Burks, J. (2002). “Mesowest: Cooperative mesonets in the western United States.” *Bulletin of the American Meteorological Society*, American Meteorological Society, 83(2), 211–226.

Irwin, H., and Peeters, M. (1980). *An Investigation of the Aerodynamic Stability of Slender Sign Bridges, Calgary*. National Research Council Canada, Calgary.

Johns, K. W., and Dexter, R. J. (1999). “Truck-Induced Wind Loads on Highway Sign Support Structures.” *1999 New Orleans Structures CongressStructural Engineering Institute of American Society of Civil Engineers, Structural Association of Alabama, National Council of Structural Engineers Associations, Florida Structural Engineers Association, Louisiana Sect*, New Orleans.

Kacin, J., Rizzo, P., and Tajari, M. (2010). “Fatigue analysis of overhead sign support structures.” *Engineering structures*, Elsevier, 32(6), 1659–1670.

Kaczinski, M. R., Dexter, R. J., and Van Dien, J. P. (1998). *NCHRP Report 412: Fatigue-Resistant Design of Cantilevered Signal, Sign and Light Supports*. *NCHRP Report 412*, Washington DC.

Koenigs, M. T., Botros, T. A., Freytag, D., and Frank, K. H. (2003). *Fatigue strength of signal mast arm connections*. Austin.

Lahiri, B. B., Bagavathiappan, S., Saravanan, T., Rajkumar, K. V, Kumar, A., Philip, J., and Jayakumar, T. (2011). “Defect detection in weld joints by infrared thermography.” *Proceedings of the International Conference on Non Destructive Evaluation for Steel and Allied Industries*, Jamshedpur, India.

Li, X., Whalen, T. M., and Bowman, M. D. (2006). *Fatigue Strength and Evaluation of Sign Structures, Volume 1: Analysis and Evaluation*. *Joint Transportation Research Program*, West Lafayette.

Ljumanovic, L. (2010). “Low cost passive dampers for highway traffic signs.” University of

Iowa.

Markow, M. J. (2007). *Managing selected transportation assets: Signals, lighting, signs, pavement markings, culverts, and sidewalks*. Transportation Research Board.

McDonald, J. R., Mehta, K. C., Oler, W., and Pulipaka, N. (1995). *Wind load effects on signs, luminaires and traffic signal structures*. *Texas Department of Transportation*, Lubbock.

McManus, P. S., Hamilton III, H. R., and Puckett, J. A. (2003). "Damping in cantilevered traffic signal structures under forced vibration." *Journal of Structural Engineering*, American Society of Civil Engineers, 129(3), 373–382.

"Metal Fatigue Solutions™." (n.d.). <https://metal-fatigue-solutions.com/crackchek-retrochek-retrofit-verification> (Jan. 13, 2021).

Miner, M. A. (1945). "Cumulative fatigue damage." *Journal of applied mechanics*, 12(3), A159–A164.

Pebesma, E., and Bivand, R. S. (2005). "S classes and methods for spatial data: the sp package." *R news*, 5(2), 9–13.

Pebesma, E. J. (2004). "Multivariable geostatistics in S: the gstat package." *Computers & geosciences*, Elsevier, 30(7), 683–691.

Peiffer, J. P., Puckett, J. A., and Erikson, R. G. (2008). *Fatigue testing of ring-stiffened traffic signal structures*. *Final Rep. No. FHWA-WY-08-05F*, Laramie.

Price, P. (1956). "Suppression of the fluid-induced vibration of circular cylinders." *Journal of the Engineering Mechanics Division*, ASCE, 82(3), 1–22.

Pulipaka, N., Sarkar, P. P., and McDonald, J. R. (1998). "On galloping vibration of traffic signal structures." *Journal of Wind Engineering and Industrial Aerodynamics*, Elsevier, 77, 327–336.

Roy, S., Park, Y. C., Sause, R., Fisher, J. W., and Kaufmann, E. J. (2011). *Cost-effective connection details for highway sign, luminaire, and traffic signal structures*.

"RStudio | Open source & professional software for data science teams - RStudio." (n.d.). <https://rstudio.com/> (Jan. 13, 2021).

Scruton, C., and Walshe, D. E. J. (1957). "A means for avoiding wind-excited oscillations of structures with circular or nearly circular cross section, natl." *Phys. Lab.(UK), Aero Rep*, 335.

Shepard, D. (1968). "A two-dimensional interpolation function for irregularly-spaced data."

Proceedings of the 1968 23rd ACM national conference, 517–524.

Shull, P. J. (2016). *Nondestructive evaluation: theory, techniques, and applications*. CRC press.

Simiu, E., and Scanlan, R. H. (1996). *Wind's effects on structures: Fundamentals and applications to design*. John Wiley & Sons, Nashville, TN.

South, J. M. (1994). *Fatigue analysis of overhead sign and signal structures*. Illinois. Dept. of Transportation. Bureau of Materials and Physical Research.

Spencer, F. W. (1996). *Visual Inspection Research Project Report on Benchmark Inspections.* SANDIA NATIONAL LABS ALBUQUERQUE NM AGING AIRCRAFT NDI VALIDATION CENTER.

"Standard Specifications & Standard Drawings | UDOT." (n.d.). <https://www.udot.utah.gov/connect/business/standards/> (Jan. 13, 2021).

"Synoptic Data." (n.d.). <https://synopticdata.com/> (Jan. 13, 2021).

Team, R. C., and DC, R. (2019). "A language and environment for statistical computing. Vienna, Austria: R Foundation for Statistical Computing; 2012." *URL https://www. R-project. org*.

Vellozzi, J., and Cohen, E. (1970). "Dynamic response of tall flexible structures to wind loading." *Building Science Series 30, Wind Loads on Buildings and Structures*, 115–128.

Vrana, J., Goldammer, M., Baumann, J., Rothenfusser, M., and Arnold, W. (2008). "Mechanisms and models for crack detection with induction thermography." *AIP conference Proceedings*, American Institute of Physics, 475–482.

Wickham, H., Averick, M., Bryan, J., Chang, W., and McGowan, L. D. (2019). "Welcome to the tidyverse." *Journal of Open Source Software*, 4(43), 1686.

Wieghaus, K. T., Mander, J. B., and Hurlebaus, S. (2017). "Damage avoidance solution to mitigate wind-induced fatigue in steel traffic support structures." *Journal of Constructional Steel Research*, Elsevier, 138, 298–307.

Xiao, Z.-G., and Yamada, K. (2003). "Fatigue evaluation of steel post structures." *STRUCTURAL ENGINEERING/EARTHQUAKE ENGINEERING*, Japan Society of Civil Engineers, 20(2), 119s-130s.

Zuo, D., and Letchford, C. W. (2010). "Wind-induced vibration of a traffic-signal-support structure with cantilevered tapered circular mast arm." *Engineering Structures*, Elsevier, 32(10), 3171–3179.

Zuo, D., Smith, D. A., and Mehta, K. C. (2014). "Experimental study of wind loading of

rectangular sign structures.” *Journal of Wind Engineering and Industrial Aerodynamics*, Elsevier, 130, 62–74.